

**THE COMPOSITION AND ORIGIN OF HYDROTHERMAL FLUIDS  
IN A NYF-TYPE GRANITIC PEGMATITE, SOUTH PLATTE DISTRICT, COLORADO:  
EVIDENCE FROM LA-ICP-MS ANALYSIS OF FLUORITE-  
AND QUARTZ-HOSTED FLUID INCLUSIONS**

JOEL E. GAGNON<sup>§</sup>

*Department of Earth and Planetary Sciences, McGill University, Montreal, Quebec H3A 2A7, Canada*

IAIN M. SAMSON AND BRIAN J. FRYER

*Department of Earth Sciences, University of Windsor, Windsor, Ontario N9B 3P4, Canada*

ANTHONY E. WILLIAMS-JONES

*Department of Earth and Planetary Sciences, McGill University, Montreal, Quebec H3A 2A7, Canada*

ABSTRACT

Hydrothermal fluorite–rare-earth-element REE mineralization occurs in the zoned Oregon No. 3 (niobium–yttrium–fluorine) granitic pegmatite (NYF-type) hosted by the Proterozoic Pikes Peak granite in north-central Colorado. The mineralization comprises secondary albite, fluorite and REE minerals (predominantly samarskite and fergusonite) that replace primary pegmatitic core-zone quartz, core-margin zone fluorite and wall-zone quartz and microcline perthite. Primary fluid inclusions in hydrothermal, purple, white and colorless fluorite and secondary and pseudosecondary inclusions in pegmatitic core-zone quartz were analyzed using microthermometry and laser-ablation ICP–MS. Such analyses of fluid inclusions in fluorite are problematic owing to compositional complexity, poor absorbance of energy, and the presence of cleavage. However, representative and quantitative analyses were made using a combination of a constricted laser beam, a traversed opening technique, and by correcting for a contribution to the fluid-inclusion signal by the host. Microthermometric and LA–ICP–MS analyses indicate that four assemblages of compositionally distinct fluid inclusions occur in core-zone quartz (fluids F1 through F3) and hydrothermal purple, white and colorless fluorite (fluids F2 and F4). Fluids F1, F2, and F3 are represented by secondary and pseudosecondary L–V and L–V–H inclusions in quartz and primary(?) L–V–H inclusions in white fluorite. These inclusions have homogenization temperatures of 93 to 149°C and contain moderate- to high-salinity (22 to 29 equiv. wt.% NaCl) fluids that can be characterized as Na + K + Sr + Ba ± Ca solutions. These three fluids (F1, F2, and F3) could not be distinguished from one another using microthermometry. They do have distinct chemical characteristics that are apparent from the LA–ICP–MS data; F2 contains detectable concentrations of Ca, and F1 and F3 do not. Fluid F4 is represented by primary L–V inclusions in purple, white and clear fluorite. These inclusions have homogenization temperatures of 81 to 114°C and comprise a low-salinity (9 to 13 equiv. wt.% NaCl) fluid that can be characterized as a Na + K + Sr + Ba solution. Only F4 appears to have been directly involved in the formation of the fluorite–REE mineralization, and these inclusions, particularly those hosted by purple fluorite, contain the highest concentrations of REE, Y, Th and U. Some compositional variation shown by F2, however, can be explained by either wall-zone albitization, which accompanies hydrothermal fluorite–REE mineralization, or by fluorite dissolution. Modeling of the fluid–rock reaction indicates that all four fluids appear to have been derived from within the pegmatite, during its later stages of crystallization. Fluorite–REE mineralization appears to have occurred at relatively constant T and pH, largely as a result of mixing of Ca liberated from the pegmatite wall-zone during albitization in the presence of an F-bearing hydrothermal fluid.

*Keywords:* granite, NYF-type pegmatite, rare-earth elements, quartz, fluorite, fluid inclusion, LA–ICP–MS, fluid–rock reaction, model, South Platte District, Colorado.

SOMMAIRE

Nous avons étudié un exemple de minéralisation hydrothermale en fluorite et terres rares dans la pegmatite granitique Oregon No. 3 de type NYF (niobium–yttrium–fluorine), associée au batholite protérozoïque de Pikes Peak, dans la partie nord-centrale du Colorado. La minéralisation comporte une association d'albite secondaire, fluorite et des minéraux de terres rares (surtout samarskite et fergusonite) qui remplace le quartz du coeur de la pegmatite, la fluorite à la bordure du coeur, et le quartz et le

<sup>§</sup> E-mail address: jgagnon@uwindsor.ca

microcline perthitique dans la zone externe de la pegmatite. Les inclusions fluides primaires dans la fluorite hydrothermale violette, blanche et incolore, et secondaires et pseudosecondaires dans le quartz du coeur du massif, ont été analysées par microthermométrie et par ablation au laser avec un appareil ICP-MS. De telles analyses d'inclusions fluides dans la fluorite sont difficiles à cause de la complexité compositionnelle, le faible taux d'absorption d'énergie, et la présence de clivage. Toutefois, des résultats représentatifs et quantitatifs ont été obtenus en utilisant un faisceau de laser confiné, une technique d'ouverture par des inclusions par traverses, et des corrections pour la contribution au signal par le minéral hôte. Les analyses microthermométriques et les analyses LA-ICP-MS indiquent que quatre assemblages d'inclusions fluides distincts en composition sont présents dans le quartz du coeur (fluides F1 à F3) et dans la fluorite hydrothermale violette, blanche et incolore (fluides F2 et F4). Les fluides F1, F2, et F3 sont représentés par les inclusions secondaires et pseudosecondaires L-V et L-V-H dans le quartz et par les inclusions primaires (?) L-V-H dans la fluorite blanche. Ces inclusions s'homogénéisent entre 93 to 149°C et contiennent une saumure à salinité de modérée à élevée (entre 22 et 29% de NaCl équiv.) que l'on peut traiter de solutions à Na + K + Sr + Ba ± Ca. Il est impossible de distinguer les trois fluides F1, F2, et F3 par microthermométrie. En revanche, ils sont distincts selon les données LA-ICP-MS; F2 contient des concentrations décelables de Ca, tandis que F1 et F3 en ont pas. Le fluide F4 est représenté par des inclusions primaires L-V dans la fluorite violacée, blanche et incolore. Ces inclusions s'homogénéisent entre 81 et 114°C et contiennent un fluide à faible salinité (9 à 13% de NaCl équiv.) que l'on peut traiter de solution à Na + K + Sr + Ba. Seul F4 semble avoir été impliqué dans la formation de la minéralisation à fluorite + terres rares. Ces inclusions, particulièrement celles dans la fluorite violacée, contiennent les teneurs les plus élevées en terres rares, Y, Th et U. Une partie de la variabilité de F2, toutefois, peut s'expliquer soit par albitisation de la zone de bordure, qui accompagne la minéralisation, soit par dissolution de la fluorite. Une simulation de la réaction entre fluide et roche montre que les quatre fluides semblent avoir été dérivés de la pegmatite même, au cours des stades tardifs de sa cristallisation. La minéralisation semble avoir eu lieu à T et pH relativement constants, surtout à cause d'un mélange de Ca libéré des parois de la pegmatite suite à une albitisation en présence d'une phase fluide fluorée.

(Traduit par la Rédaction)

*Mots-clés:* granite, pegmatite de type NYF, terres rares, quartz, fluorite, inclusion fluide, analyses LA-ICP-MS, réaction roche-eau, modèle, district de South Platte, Colorado.

## INTRODUCTION

Hydrothermal processes responsible for fluorite – rare-earth element (REE) mineralization have been documented from a number of localities (*e.g.*, Salvi & Williams-Jones 1992, Williams-Jones *et al.* 2000, Samson *et al.* 2001, Bühn *et al.* 2003), including mineralization hosted by (niobium – yttrium – fluorine) granitic pegmatites in the South Platte District, Colorado (*e.g.*, Simmons & Heinrich 1980, Levasseur & Samson 1996, Levasseur 1997, Gagnon *et al.* 2002). Detailed mapping and description of the mineralogy of the South Platte NYF-type granitic pegmatites and fluorite-REE mineralization have been conducted, but only limited microthermometric data are available on the fluids responsible for the mineralization (*e.g.*, Simmons & Heinrich 1980, Levasseur 1997). Furthermore, very little quantitative information is available on the composition of the fluids responsible for the formation of hydrothermal REE mineral deposits in general.

Laser ablation – inductively coupled plasma – mass spectrometry (LA-ICP-MS) has been used in a number of studies to quantitatively determine elemental concentrations within individual fluid inclusions (*e.g.*, Audétat *et al.* 1998, 2000, Shepherd *et al.* 1998, Günther *et al.* 1998, Heinrich *et al.* 1999, Ulrich *et al.* 1999, Müller *et al.* 2001, Landtwing *et al.* 2002). These investigators have concentrated on relatively large fluid inclusions (greater than 30 µm in diameter) hosted by quartz, a mineral that is compositionally simple and lacks cleavage. In many geological settings, including that of the

fluorite-REE mineralization in the South Platte District, the fluid inclusions of interest are small (1 to 15 µm) and are hosted by compositionally complex minerals that may have well-developed cleavages (*e.g.*, fluorite). Collectively, these fluid inclusion and host-mineral attributes make analysis by LA-ICP-MS more problematic. Analytical procedures and data-reduction strategies applicable to larger fluid inclusions in compositionally simple host-minerals are not necessarily valid.

In this study, we discuss a procedure adapted to laser sampling of fluid inclusions hosted by primary magmatic quartz and secondary hydrothermal fluorite from the Oregon No. 3 pegmatite in the South Platte district, Colorado. Using this method, relatively small fluorite- and quartz-hosted fluid inclusions have been analyzed, and the potential effect of host-mineral composition on fluid-inclusion composition quantitatively removed. The LA-ICP-MS analyses of fluid inclusions have been used to constrain: 1) the character and potential source(s) of the fluid(s) responsible for the fluorite-REE mineralization, and 2) the timing of this mineralization relative to formation of the associated pegmatites.

## FLUORITE-REE MINERALIZATION, SOUTH PLATTE, COLORADO

### *The Oregon No. 3 pegmatite*

The fluorite-REE mineralization in the South Platte District occurs within complex, concentrically zoned, REE-F-Y-Nb-U-enriched granitic pegmatites hosted

by the Proterozoic, anorogenic Pikes Peak granitic batholith in north-central Colorado (Hedge 1970, Simmons & Heinrich 1970, 1980, Simmons *et al.* 1987) (Fig. 1). Over 50 pegmatites occur within the reversely zoned northern portion of the batholith, which is referred to as the Buffalo Park Intrusive Center. With one ex-

ception, all of the bodies of pegmatite are hosted within the outer, granitic portion of the batholith rather than the quartz monzonite core. Generally, the pegmatites are characterized by high concentrations of fluorine, REE and ferric iron (as hematite) (Simmons & Heinrich 1980).

Some of the zoned pegmatites contain secondary, hydrothermal fluorite and REE minerals (Simmons &

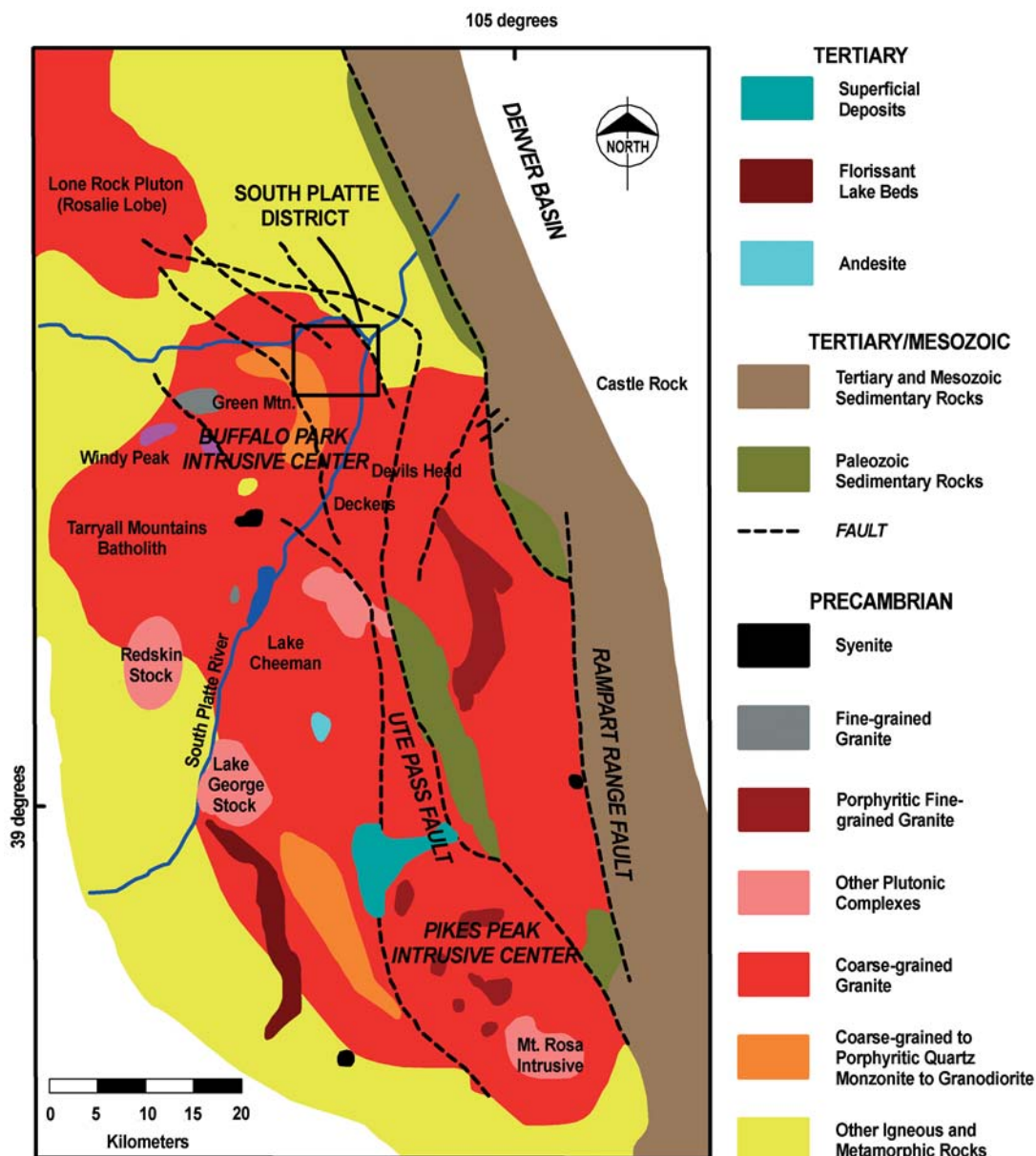


FIG. 1. Geology of the Proterozoic Pikes Peak batholith, north-central Colorado (modified from Simmons & Heinrich 1980). Over 50 bodies of granitic pegmatite occur in the South Platte District, which is situated in the granitic Buffalo Park Intrusive Center.

Heinrich 1970, 1980, Brewster 1986). The Oregon No. 3 pegmatite is approximately 200 m long by up to 90 m wide and is crudely elliptical. This pegmatite is moderate in size and relatively simple compared with other pegmatites in the district, as it comprises only three primary zones: a quartz – microcline perthite – biotite wall zone, a fluorite core-margin zone, and a quartz core zone, and one secondary zone, a core-margin zone of hydrothermal replacement (Fig. 2). Primary, magmatic, core-margin fluorite and secondary, hydrothermal, replacement-type mineralization hosted by the Oregon No. 3 pegmatite are some of the best examples of this mineralization in the district.

The volumetrically largest unit of the pegmatite is the wall zone, which consists of intergrown quartz and microcline perthite with accessory biotite. The core-margin zone, which is up to 25 cm thick, contains massive, coarse-grained green fluorite. It typically occurs as discontinuous, scattered pods and irregular bodies along the outer edge of the quartz core. Primary fluorite occurs rarely as crudely formed, idiomorphic crystals (Simmons & Heinrich 1980). The core zone of the Oregon No. 3 pegmatite consists almost entirely of white and clear quartz. Vugs, ranging from less than 25 mm to meters in diameter, occur within the core and contain large, well-formed crystals of smoky quartz. In some cases, these crystals are in excess of 30 cm wide and up to 150 cm long (Simmons & Heinrich 1980). On the basis of surface exposure, the wall, core-margin and core zones are estimated to comprise approximately 63, 2 and 35% of the pegmatite, respectively (Simmons & Heinrich 1980).

#### *Hydrothermal fluorite–REE mineralization*

Secondary, hydrothermal mineralization occurs at the border between the core zone and wall zone, principally in the wall zone or core-margin fluorite, and comprises, in decreasing order of abundance, albite, quartz, fluorite, hematite, REE minerals (predominantly samarskite and fergusonite) and white mica (Simmons & Heinrich 1980). Hydrothermal mineralization is concentrated near the upper part of the pegmatite. The latest fluorite preferentially replaces primary green fluorite in the primary core-margin zone. Albite, along with fluorite and REE minerals, typically replaces wall-zone perthite, and comprises either cross-cutting bladed aggregates of albite or, more predominantly, patchy, granular replacements (Simmons & Heinrich 1980).

Three types of hydrothermal fluorite replace minerals of the core-margin zone within the Oregon No. 3 pegmatite. These are, in decreasing relative abundance, purple, white and colorless fluorite, and these three variants occur as stockwork and patchy replacements, from 1 mm to several cm wide, within green fluorite and wall-zone feldspar. Purple fluorite commonly contains inclusions of REE minerals (samarskite, fergusonite, monazite, xenotime, gadolinite, allanite, yttrifluorite

and bastnäsite), hematite and quartz (Simmons & Heinrich 1980) and, in some instances, is opaque owing to the high proportion of mineral inclusions. Patchy white fluorite replaces green fluorite and, in some instances, occurs peripherally to veins and patches of purple fluorite. Purple, white and colorless fluorite also occur as vug fillings (Simmons & Heinrich 1980). Paragenetically, purple fluorite is earliest and is mantled by later white or zoned white and purple fluorite. Purple and white fluorite commonly grade into one another or are intergrown as patchy replacements of green fluorite. Colorless fluorite postdates purple and white fluorite, as it occurs interstitially to euhedral crystals of purple fluorite, lining vugs between purple and white fluorite euhedra, and as veinlets cross-cutting purple and white fluorite (Levasseur 1997).

REE minerals (principally samarskite and fergusonite) commonly occur as coarser-grained aggregates, associated primarily with purple and less commonly with white fluorite, within albitized K-feldspar (Simmons & Heinrich 1980, Levasseur 1997). These textural relationships indicate that albitization of K-feldspar and deposition of relatively coarse-grained REE minerals accompanied the deposition of purple fluorite.

#### FLUID-INCLUSION PETROGRAPHY

Three samples from the Oregon No. 3 pegmatite were chosen for detailed analysis of the fluid inclusions. The first sample, RL-94-55b, was collected from the north-central edge of the core, from a hydrothermally altered portion of the core-margin zone. The sample comprises green, purple, white and colorless fluorite, REE minerals, quartz and hematite. Patches of relict, primary, green fluorite and K-feldspar occur in a matrix of predominantly purple and white fluorite. The purple and white fluorite grade into one another, and patches of dark purple fluorite occur within white fluorite and as stockwork replacements within green fluorite. The second sample, RL-94-60, which comprises coarse, primary clear quartz with minor hematite stains, was collected from the approximate center of the quartz core. The third sample, RL-94-63, was collected at the southern edge of the core, from a hydrothermally altered portion of the core-margin zone. The sample comprises primarily quartz and pink K-feldspar that have been partially replaced by dark purple and white fluorite. The locations of the three samples are shown in Figure 2.

Fluid-inclusion petrography was performed on chips taken from doubly polished wafers prepared from core-zone quartz (RL-94-60) and hydrothermal purple (RL-94-63), white (RL-94-55b and RL-94-63), and colorless (RL-94-55b) fluorite. The samples were evaluated using standard petrographic techniques, and fluid-inclusion assemblages were classified according to the types and proportions of phases present in the fluid inclusions at room temperature. Two principal types of fluid inclusion were identified: 1) aqueous, liquid–vapor

(L–V) inclusions, hosted by core-zone quartz (Fig. 3A) and hydrothermal purple, white and colorless fluorite (Fig. 3B), and 2) aqueous liquid – vapor – halite (L–V–H) inclusions, hosted by core-zone quartz (Fig. 3C) and hydrothermal white fluorite. The two types of fluid inclusion identified in this study comprise a subset of the fluid inclusions previously documented within pegmatites of the South Platte district by Simmons & Heinrich (1980) and Levasseur (1997).

Aqueous L–V inclusions in purple, white and colorless fluorite are typically equant, and generally range in diameter from 5 to 30  $\mu\text{m}$ . The majority of the inclusions are, however, relatively small (less than 20  $\mu\text{m}$ ) (Fig. 3B). The inclusions typically occur either isolated from other inclusions or in clusters of 5 to 15 inclusions arranged in three-dimensional, non-planar arrays. In some instances, clusters of inclusions are concentrated in zones that parallel crystal faces or color zoning within the fluorite, indicating that the inclusions were trapped along primary growth-zones. The inclusions are dominated by liquid (estimated to be approximately 70% by volume), and the relative proportions of the phases within inclusions of a given assemblage are consistent. The occurrence, distribution and consistent phase-ratios of this fluid-inclusion assemblage indicate a primary origin for these inclusions.

Aqueous L–V inclusions in quartz mostly range in size from 5 to 40  $\mu\text{m}$ , are elongate, with aspect ratios of 2:1 to 3:1, and generally occur in clusters of greater than 10 inclusions arranged in planar arrays (Fig. 3A). The orientations of the long axes of the inclusions comprising an individual cluster are similar and parallel to the plane defined by the fluid inclusions. The L–V inclusions are dominated by liquid (estimated to be approximately 70 to 80% by volume), and the relative proportions of the phases are consistent within an individual plane of inclusions. The distribution along planes within the quartz indicates a secondary origin for these inclusions (along healed fractures), although given the large size of these crystals, a pseudosecondary origin cannot be ruled out.

Aqueous L–V–H inclusions are typically equant, generally range in size from 10 to 30  $\mu\text{m}$ , and are abundant in quartz (Fig. 3C) and rare in white fluorite. These inclusions are dominated by liquid (estimated to be approximately 70% by volume), with the vapor and solid phases occupying approximately 20 and 10% by volume, respectively. Phase proportions are generally consistent within an assemblage. The solid is interpreted to be a halite daughter crystal as it is cubic, isotropic, reacts to form hydrohalite, and consistently occupies the same percentage of the volume of an inclusion in a given assemblage. In quartz, L–V–H inclusions typically occur in clusters of greater than five inclusions arranged in planar arrays, suggesting that these fluid inclusions are secondary or pseudosecondary in origin. In white fluorite, L–V–H inclusions typically occur in clusters of less than five inclusions that do not appear to be ar-

ranged in planar arrays. The three-dimensional arrangement is consistent with a primary origin for these inclusions; the lack of any obvious color-related growth zoning in the white fluorite, however, precludes any conclusive statement being made regarding their origin. A summary of the fluid-inclusion assemblages analyzed as part of the study is provided in Table 1.

#### *Fluid-inclusion microthermometry*

Microthermometric measurements were conducted using a Linkam THMSG 600 heating–freezing stage. To reduce the risk of stretching or decrepitating the fluid inclusions, heating experiments were conducted on fluorite-hosted fluid inclusions prior to conducting cooling experiments. The salinity of the L–V inclusions was determined from the temperature of final melting of ice or hydrohalite. The salinity of the L–V–H inclusions was determined from the temperature of final dissolution of halite. The results of the microthermometric analyses are summarized in Table 2.

All of the primary L–V inclusions hosted by purple, white and colorless fluorite exhibit similar behavior of phase assemblages during heating and cooling. Upon heating, the L–V inclusions homogenize to the liquid phase at temperatures ranging from 81 to 114°C. The range of homogenization temperatures for an individual fluid-inclusion assemblage (FIA) was less than 5°C. Upon heating after freezing, first melting (*i.e.*, the eutectic temperature) was observed at between –46 and –34°C. The temperatures of final melting of hydrohalite range from –43 to –25°C (individual FIA < 9°C). Ice was the last phase to melt at temperatures ranging from –9.1 to –5.6°C, indicating that the fluorite-hosted L–V fluid inclusions have salinities ranging from 9.2 to 12.8 equivalent wt.% NaCl.

Upon heating, the vapor bubbles in white-fluorite-hosted L–V–H fluid inclusions disappear at temperatures of 104 to 108°C (individual FIA < 4°C). Homogenization by halite dissolution was observed in two inclusions at a temperature of 137°C, indicating a salinity of 29% NaCl equiv. Upon cooling, the inclusions froze to a mixture of ice, hydrates and halite; upon subsequent heating, first melting was observed at –58 to –22°C. The temperatures of final melting of ice range from –34.2 to –7.4°C.

Quartz-hosted, secondary L–V inclusions homogenized to the liquid phase at temperatures ranging from 93 to 126°C (individual FIA < 1°C). Upon cooling, the inclusions froze to a homogeneous solid and, upon subsequent heating, first melting was observed at approximately –26 to –20°C. Temperatures of final melting of ice ranged from –25.3 to –19.5°C, indicating that the quartz-hosted L–V fluid inclusions have salinities ranging from 22.4 to 25.6% NaCl equiv.

When heated, the vapor bubble in quartz-hosted L–V–H fluid inclusions disappears at 102 to 122°C (individual FIA < 5°C). Homogenization of the inclusions

occurs by halite dissolution at temperatures ranging from 144 to 149°C, indicating salinities of  $29.5 \pm 0.1\%$  NaCl equiv. The narrow range of halite-dissolution temperatures (5°C) of all the quartz-hosted secondary L–V–H inclusions supports the interpretation that this is a daughter mineral and not a trapped phase. Upon cooling, the inclusions froze to a mixture of ice, hydrates and halite and, upon subsequent heating, first melting was observed at –55 to –46°C. Temperatures of final melting of hydrohalite melting range from –13.1 to –12.5°C, and of melting of ice, from –39.0 to –37.8°C.

The microthermometric analyses indicate that three fluids occur within the Oregon No. 3 pegmatites: 1) a relatively low-salinity (9 to 12 wt. % NaCl equiv.) fluid represented by the primary, aqueous, L–V inclusions within purple, white and colorless fluorite, 2) a moderate-salinity (22 to 25 wt.% NaCl equiv.) fluid represented by the secondary, aqueous, L–V inclusions within quartz, and 3) a relatively high-salinity (29 wt.% NaCl equiv.) fluid represented by the primary, aqueous, L–V–H inclusions in white fluorite and secondary or pseudosecondary, aqueous, L–V–H inclusions in quartz.

### LA-ICP-MS ANALYSIS

#### Instrumentation

Laser-ablation ICP–MS analysis of fluorite- and quartz-hosted fluid inclusions was conducted at the Great Lakes Institute for Environmental Research at the University of Windsor. The facility is equipped with a non-homogenized, solid-state, 266 nm Nd-doped Y–Al garnet (Nd:YAG) laser. Analyses were performed on chips taken from doubly polished wafers and bonded to glass slides. All samples were cleaned prior to analysis by washing with distilled, deionized water and ethanol. Sample ablation was conducted in an Ar gas-filled sampling cell mounted to the stage of a modified polarizing microscope. The ablated material was transported from the ablation cell to the ICP–MS using Ar as the carrier gas. Wherever possible, fluid inclusions that occurred in assemblages, but sufficiently separated to enable analysis of individual inclusions, were selected so that replicate analyses could be performed. The ablation process was observed throughout, and the time of initiation and duration of fluid inclusion opening were recorded for use during data reduction.

Elemental analysis was performed using a Thermo-Elemental PQ3 ICP–MS, and instrument calibration was accomplished using NIST glass standard 610 (*cf.* Heinrich *et al.* 2003). The elements sought included the



FIG. 2. Plan of the Oregon No. 3 pegmatite (modified from Simmons & Heinrich 1980). This pegmatite is relatively simple compared with other zoned pegmatites in the district. There are only three primary zones: a quartz core, a fluorite – albite – REE mineral core-margin zone, and a quartz – microcline perthite – biotite wall-zone. Secondary, hydrothermal fluorite–REE mineralization occurs predominantly in the core-margin zone and the immediately adjacent parts of the wall zone.

TABLE 1. SUMMARY OF FLUID INCLUSIONS ANALYZED. OREGON No. 3 GRANITIC PEGMATITE, SOUTH PLATTE DISTRICT, COLORADO

Variety	Zone	Sample	Type	Origin
<b>Fluorite-hosted</b>				
Purple	Core-margin	RL-94-63	Aqueous L V	Primary
White	Core-margin	RL-94-63	Aqueous L V	Primary
Colorless	Core-margin	RL-94-55b	Aqueous L V H	Primary?
		RL-94-55b	Aqueous L V	Primary
<b>Quartz-hosted</b>				
Clear	Core	RL-94-60	Aqueous L–V	
	Secondary		Aqueous L V H	
	Secondary			

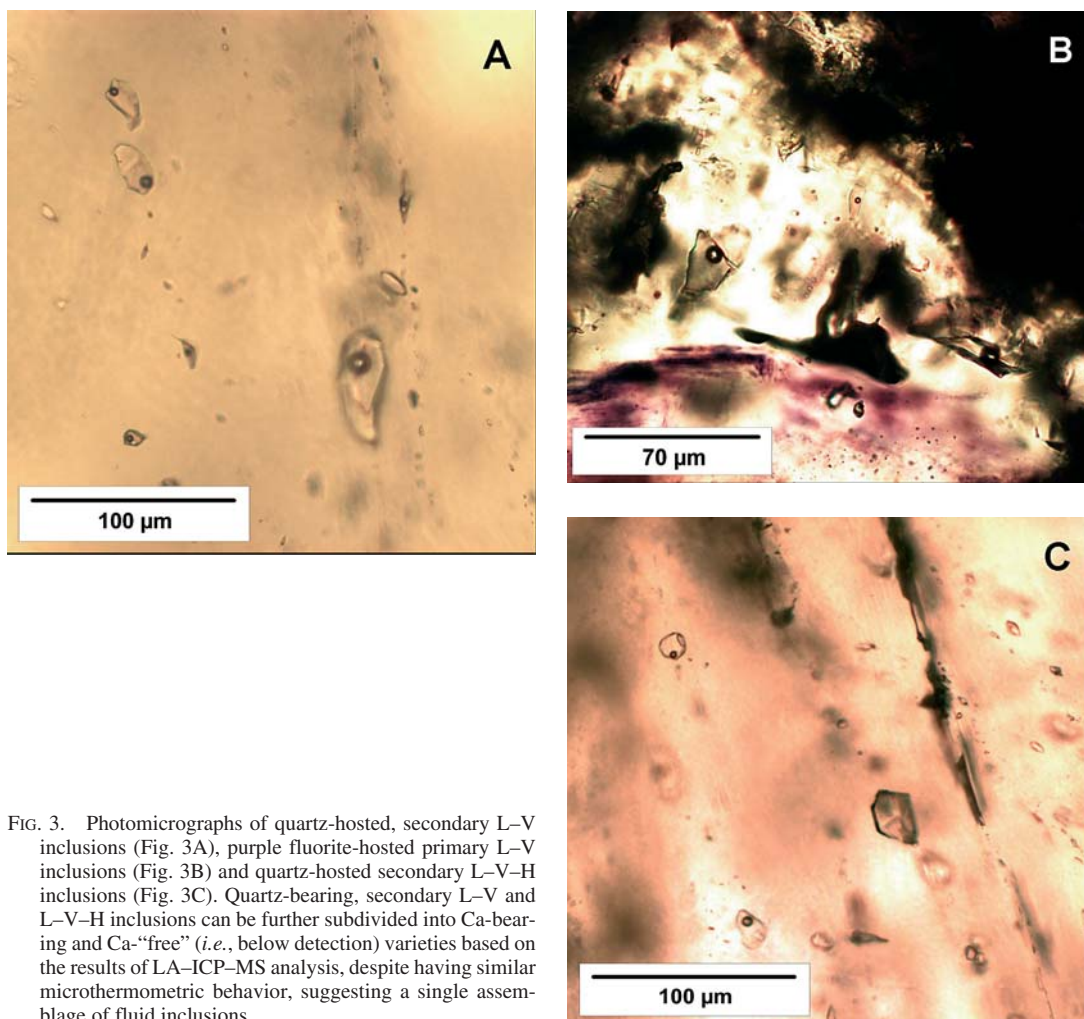


FIG. 3. Photomicrographs of quartz-hosted, secondary L-V inclusions (Fig. 3A), purple fluorite-hosted primary L-V inclusions (Fig. 3B) and quartz-hosted secondary L-V-H inclusions (Fig. 3C). Quartz-bearing, secondary L-V and L-V-H inclusions can be further subdivided into Ca-bearing and Ca-“free” (*i.e.*, below detection) varieties based on the results of LA-ICP-MS analysis, despite having similar microthermometric behavior, suggesting a single assemblage of fluid inclusions.

TABLE 2. SUMMARY OF MICROTHERMOMETRIC DATA, OREGON No. 3 GRANITIC PEGMATITE, SOUTH PLATTE DISTRICT, COLORADO

Type	Data	$T_c$	$T_m(\text{bH})$	$T_m(\text{ice})$	$T_h(\text{L-V})$	$T_m(\text{NaCl})$
<b>Fluorite-hosted</b>						
L-V	Range	-46.4 to -34.5	-43.4 to -24.7	-9.1 to -5.6	80.7 to 114.5	--
	Average	-40.8	-27.7	-7.2	96.3	--
L-V-H	Range	-57.7 to -22.4	--	-34.2 to -7.4	104.3 to 108.5	137
	Average	-38.4	--	-17.8	106.4	137
<b>Quartz-hosted</b>						
L-V	Range	-26.4 to -19.5	--	-25.3 to -19.5	92.7 to 125.5	--
	Average	-24	--	-21.1	112.6	--
L-V-H	Range	-54.8 to -46.2	-13.1 to -12.48	-39 to -37.8	101.7 to 121.9	144.3 to 148.7
	Average	-51.1	-12.8	-38.4	107.5	146.6

Footnotes: All data reported in °C. -- Indicates not applicable or not observed.

major elements most likely to be present in the inclusions, which are also required for calculations in the internal standardization (Na, K, Ca), and trace elements that are of interest in characterizing and potentially differentiating the hydrothermal fluids responsible for the formation of these deposits (Be, Sr, Y, Zr, Nb, Ba, Ce, Sm, Ho, Th and U). The list of analytes was minimized in order to maximize (optimize) the number of sweeps that could be obtained across the selected masses for a given time-interval. For example, limiting the list of analytes to 11 masses resulted in sweep times of approximately 140 ms, enabling the collection of approximately 35 mass scans for a 5-s-long signal. A summary of the equipment specifications and general operating conditions of the instrument used during analysis of the fluid inclusions is provided in Table 3. Additional details pertaining to the instrument specifications, operation and calibration are presented in Gagnon *et al.* (2003a).

#### Sampling technique

Relatively large fluid inclusions hosted by minerals that a) readily absorb laser energy, b) have a relatively high tensile strength, and c) lack structural discontinuities, such as cleavages, can generally be sampled using laser ablation without significant difficulty. Fluid inclusions hosted by minerals that do not have these characteristics, however, such as fluorite, may require specialized sampling procedures to ensure representative sampling of the fluid inclusion's contents. Furthermore, most authors of previous LA-ICP-MS studies of fluid inclusions have used a homogenized, 193 nm ArF Excimer laser and a stepwise opening technique to conduct quantitative analyses of individual, relatively large, quartz-hosted fluid inclusions (*e.g.*, Audétat *et al.* 1998, 2000, Günther *et al.* 1998, Heinrich *et al.* 1999, Ulrich *et al.* 1999). In contrast, our facility is equipped with a non-homogenized 266 nm Nd-YAG laser and, when sampling some minerals, the Gaussian distribution of energy of the laser beam can result in differential ablation-characteristics across the diameter of the beam,

potentially causing fracturing of the sample at the low-energy edge of the beam, and resulting in uncontrolled opening of the fluid inclusions and non-representative sampling of the contents (Gagnon *et al.* 2003a). Beam homogenization is not an option for this system, owing to the significant reduction in laser power and coherence associated with homogenization.

To overcome the drawbacks of the non-homogenized 266 nm Nd:YAG laser for the analysis of individual fluid inclusions in fluorite, fixed-diameter beam constrictors (*i.e.*, pinholes) are used to reduce the size of the laser beam. If precisely centered on the laser beam, the constrictors trim the beam to a size that is appropriate for the analysis of smaller inclusions. This trimming also is important because it removes the lower-energy, outer portion of the laser beam that may contribute to the differential ablation characteristics of the Gaussian energy distribution, and preserves the high-energy core of the beam, which improves ablation characteristics of poorly absorbing minerals such as fluorite. The system is relatively simple (Fig. 4), and we did not experience the losses in coherence and reflectance inherent in expanding and homogenizing laser beams using complex arrays of lenses.

Two pinholes arranged in series enable stepwise opening of the fluid inclusions. However, the fluorite-hosted fluid inclusions analyzed in this study are relatively small (generally 10 to 15  $\mu\text{m}$  in maximum diameter); consequently, stepwise opening of the inclusions was neither necessary nor desirable, as the lowest possible limits of detection were sought. Direct opening of the fluorite-hosted fluid inclusions (*i.e.*, initiating ablation directly over the inclusion to be analyzed) was initially attempted; however, the sudden thermal and mechanical shock to the sample resulting from initiation of ablation over the inclusions commonly resulted in fracturing of the sample, premature decrepitation of the fluid inclusions, and loss of the contents of the fluid inclusion. Greater success was achieved by conducting "traversed opening" of the fluid inclusions. In a traversed opening, ablation was initiated at a distance of approximately 50 to 100  $\mu\text{m}$  from the fluid inclusion using a beam diameter approximately equal to the diameter of the fluid inclusion to be analyzed. After a stable process of ablation was established, the surface of the sample was traversed using a computer-controlled, motorized X-Y-Z stage until the laser was immediately over the fluid inclusion, at which time traversing was discontinued, and the beam was allowed to "drill" into the sample. Fluid inclusions up to 150  $\mu\text{m}$  below the surface of the sample could be analyzed; however, most inclusions were 30 to 100  $\mu\text{m}$  deep. This method of analysis was designed to provide the most controlled ablation for the design of the system, the primary objective being representative sampling of the entire contents of the fluid inclusion. Through integration of the entire fluid-inclusion signal, the resultant analyses reflect the bulk composition of the fluid, in-

TABLE 3. SUMMARY OF LA-ICP-MS INSTRUMENT SPECIFICATIONS AND OPERATING CONDITIONS AT THE GREAT LAKES INSTITUTE, UNIVERSITY OF WINDSOR

Laser-sampling system	ICP MS
Manufacturer: Continuum	Manufacturer: ThermoElemental
Model: Surelite 1	Model: PQ3
Wavelength: 266 nm	Mode: peak-jumping
Energy / pulse: 1 mJ	Dwell time / isotope: 10 ms
Mode: Q-switched	Sensitivity (solution): $3 \times 10^8$
Frequency: 20 Hz	counts / s / ppm (U)
Pulsewidth: 4 to 6 ns scan	Scan time: approximately 150 ms /
Laser-spot diameter (at sample): 10–15 $\mu\text{m}$	

clusive of all solid, liquid and gas phases present in the inclusions, and the lowest possible limits of detection.

The combination of beam constriction and traversed opening significantly improved the proportion of fluo-rite-hosted fluid inclusions that could be successfully analyzed using our non-homogenized 266 nm laser

beam, from less than 50% using direct opening to 80 to 90% using beam constriction and traversed opening.

*Data reduction*

Conversion of the transient ICP-MS output data (integrated counts/second) to concentration units ( $\mu\text{g/g}$ )

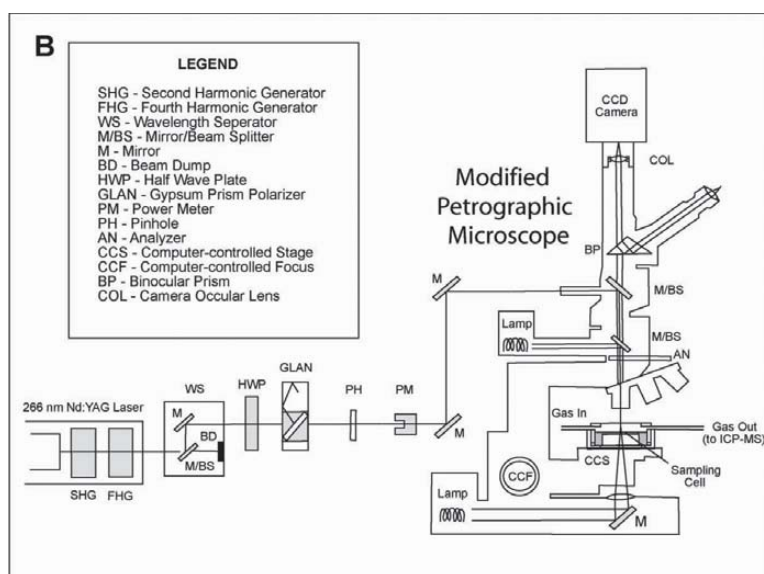
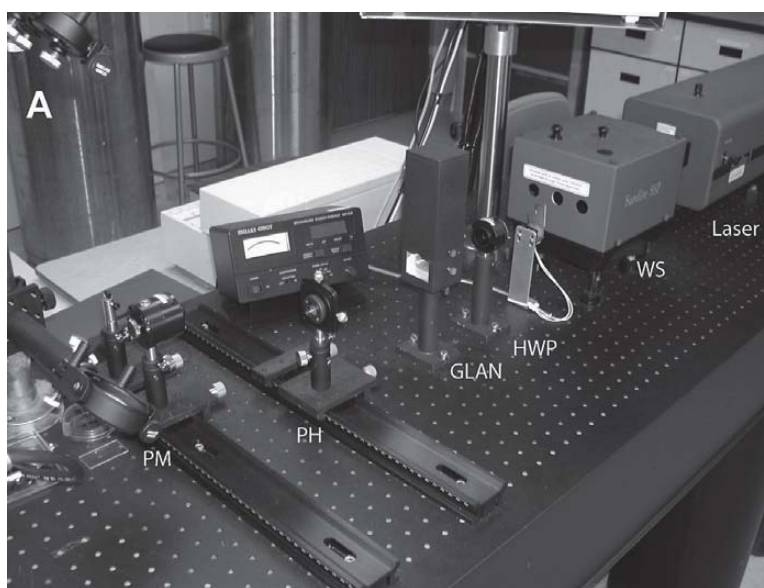
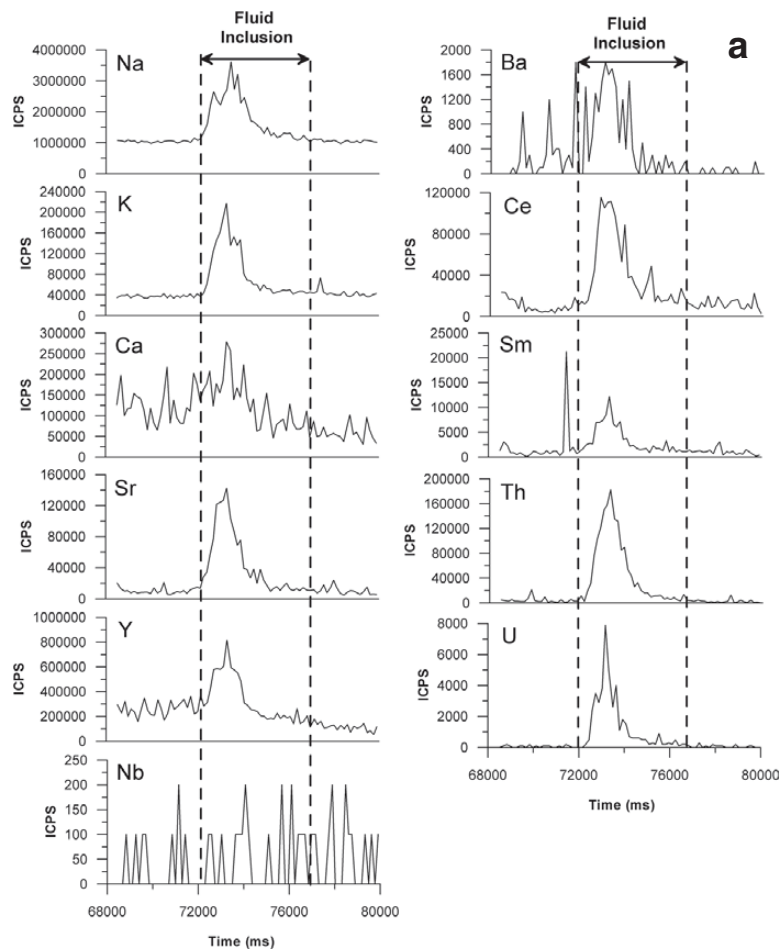


FIG. 4. Photograph (Fig. 4A) and schematic diagram (Fig. 4B) of LA-ICP-MS facility at the Great Lakes Institute for Environmental Research, University of Windsor.

was accomplished using the method described in Gagnon *et al.* (2003a). In general, the method differs from that used by others for the analysis of melt and fluid inclusions (*e.g.*, Halter *et al.* 2002, Heinrich *et al.* 2003) in that: a) rather than applying a single relative-sensitivity factor (RSF) calculated for Na to all elements, a correction factor is calculated for each element in the fluid inclusion, and b) a ratioing procedure is applied to the data from fluorite-hosted inclusions to remove host-mineral contributions to the fluid-inclusion signal that are not removed by simple subtraction of background. The data-reduction procedure for fluorite- and quartz-hosted inclusions consists of: 1) calculation and subtraction of the average background (*i.e.*, instrument and host mineral) from the spectra, 2) determination of the significance of the fluid-inclusion spectra (*i.e.*, detection-limit screening), 3) integration of spectral peak-area, and 4) calculation of the composition of the fluid inclusion. Data from fluorite-hosted fluid inclusions are also ratioed against Ca after background

subtraction to remove host-mineral contributions (Gagnon *et al.* 2003a).

For spectra of elements that exhibit non-zero backgrounds, the average count-rates obtained during measurement of the pre-ablation signal (*i.e.*, combined instrument and gas-blank background) or the pre-inclusion host mineral (*i.e.*, host-mineral background) were subtracted from the count rates obtained during fluid-inclusion analysis. The spectra were then evaluated to determine whether the count rates obtained for Na over the duration of the fluid-inclusion analysis exceed the mean background plus  $3\sigma$  count rates obtained for the host mineral (*i.e.*, whether the count rates obtained for Na in the fluid-inclusion signal are statistically significantly different from the background count-rates determined on the host mineral) (*cf.* Longerich *et al.* 1996). If the Na count rates were determined to be statistically insignificant from the host, the analytical data were discarded; otherwise, all other element spectra for the fluid inclusion were evaluated in a similar manner and, if the



count rates during fluid-inclusion analysis were found to be statistically significant, further data-reduction procedures were applied.

It is impossible to conduct laser-ablation sampling of fluid inclusions without some of the host mineral being included in the sample that is introduced to the ICP-MS. For fluorite-hosted fluid inclusions, background subtraction often is inadequate to remove a host-mineral contribution to the fluid-inclusion signal. Therefore, the background-subtracted data obtained from fluorite-hosted fluid inclusions were further corrected by dividing the count rate obtained for each element for a single mass-scan by the count rate obtained for Ca for the same mass-scan. Calcium was selected because it is a major constituent of the host fluorite and is expected to have low concentrations owing to the low

solubility of fluorite in fluids with a salinity comparable to that of the fluorite-hosted inclusions (Richardson & Holland 1979).

Uncorrected and corrected spectra, obtained for an approximately 12  $\mu\text{m}$ , primary, L-V inclusion in purple fluorite, are illustrated in Figure 5. Subtraction of the instrumental and background count-rates of the host mineral was inadequate to correct for the host-mineral contribution in the early part of the spectra, as indicated by the residual spectral peak for Ca (Fig. 5A). A fluid inclusion hosted by fluorite cannot have a higher concentration of Ca than the host; therefore, the part of the Ca spectrum corresponding to the fluid inclusion should not exhibit a positive peak. The uncorrected spectra suggest that this fluid inclusion contains Na, K, Ca, Sr, Y, Ba, Ce, Sm, Th and U; however, the corrected spectra

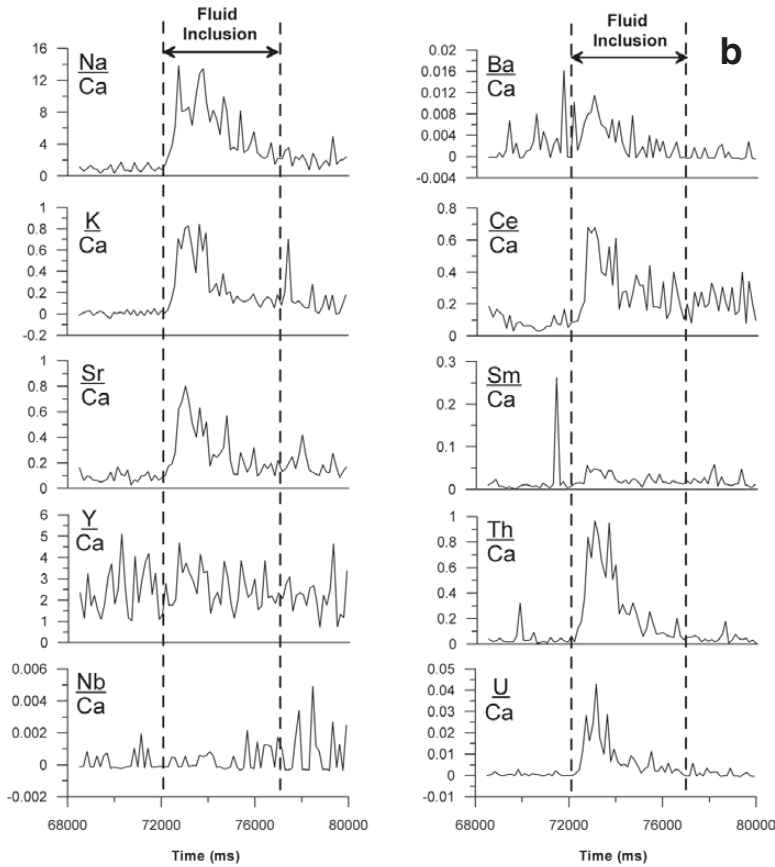


FIG. 5. A. LA-ICP-MS spectra of a fluorite-hosted L-V fluid inclusion that have had instrument and host-mineral backgrounds subtracted. These spectra suggest that this inclusion contained Na, K, Ca, Sr, Y, Ba, Ce, Sm, Th and U. B. The same spectra after individual element count-rates have been ratioed against the count rates obtained for Ca. These spectra show that Ca and Y in the uncorrected spectra were contributed to the fluid-inclusion signal by the host fluorite. Calculation of fluid-inclusion compositions from the uncorrected data would therefore result in erroneous results.

show that Ca and Y were contributed to the fluid-inclusion signal by the host fluorite (Fig. 5B). The differences between the areas of corrected and uncorrected spectral peaks indicate that determination of element concentrations without initially carrying out a host-mineral correction will result in erroneous results (Gagnon *et al.* 2003a).

To obtain quantitative data on the composition of an inclusion, it is first necessary to obtain, as accurately as possible, an estimate of the concentration of Na in the inclusion using microthermometric analysis. The concentration of Na, as microthermometric analysis ( $\text{Na}_{\text{MT}}$ ), was used as an internal standard for the calculation of the abundances of all other elements within the fluid inclusions. Ideally, interpretation of the microthermometric data to obtain  $\text{Na}_{\text{MT}}$  will account for the abundance of other major electrolytes in the inclusions, *i.e.*, those electrolytes that would have a significant effect on measurements such as  $T_{\text{m}}(\text{ice})$  and  $T_{\text{m}}(\text{NaCl})$  (*cf.* Heinrich *et al.* 1992). The abundance of K in all fluid inclusions in this study is negligible relative to the abundance of Na or Ca. Therefore, the phase relationships exhibited by the fluid inclusions are best interpreted using the system  $\text{H}_2\text{O}-\text{NaCl}$  (for Ca-free inclusions) or the system  $\text{H}_2\text{O}-\text{NaCl}-\text{CaCl}_2$  (for Ca-bearing inclusions). It is possible to carry out such a correction and to determine a more accurate  $\text{Na}_{\text{MT}}$  value for Ca-bearing quartz-hosted inclusions. However, a similar correction cannot be applied to fluorite-hosted inclusions because the fluid-inclusion-derived Ca signal is masked by that derived from the host mineral.

The  $\text{Na}_{\text{MT}}$  value for Ca-free inclusions was calculated using the equation of Bodnar (1993) for L-V inclusions and from the data of Sterner *et al.* (1988) for L-V-H inclusions. For quartz-hosted, Ca-bearing L-V inclusions, total salinity can be calculated using equation (2) of Oakes *et al.* (1990) and the Ca:Na ratio measured from LA-ICP-MS analyses. Heinrich *et al.* (1992) presented the following equation, based on the data of Vanko *et al.* (1988), that relates the apparent salinity of an inclusion [equivalent weight percent NaCl calculated from  $T_{\text{m}}(\text{NaCl})$  according to Sterner *et al.* (1988)] to the concentrations of NaCl and  $\text{CaCl}_2$  in L-V-H inclusions:

$$\text{Salinity}_{\text{MT}} = \text{NaCl}_{\text{MT}} \cdot \text{CaCl}_2_{\text{MT}} \quad (1).$$

This equation is, however, only valid at temperatures above 300°C. At lower temperatures, the NaCl solubility isotherms are not normal to the NaCl-H<sub>2</sub>O binary join, which is the basis for equation (1). Furthermore, the calculations of Williams-Jones & Samson (1990) suggest that below 300°C, the isotherms are curved. Therefore, for quartz-hosted L-V-H inclusions with  $T_{\text{m}}(\text{NaCl}) < 300^\circ\text{C}$ , NaCl and  $\text{CaCl}_2$  contents have to be estimated graphically using the isotherms presented by Vanko *et al.* (1988) or Williams-Jones & Samson (1990). In this case, the isotherms of Williams-Jones & Samson (1990) were used because they are better de-

fined in the temperature range of  $T_{\text{m}}(\text{NaCl})$  observed in this study (140 to 150°C).

The apportioning of a fraction of the salinity to electrolytes other than Na leads to a reduction in the  $\text{Na}_{\text{MT}}$  value, which results in a decrease in the concentrations of all other elements determined to be present in the fluid inclusion. For example, if  $\text{Na}_{\text{MT}}$  is corrected for the presence of Ca in the most Ca-rich, quartz-hosted L-V-H fluid inclusions measured in this study, the concentrations of all electrolytes detected in the inclusion (Na, K, Ca and Sr) decrease by approximately 39%. This reduction represents an extreme case, because it is based on the most Ca-rich fluid inclusion analyzed. Other inclusions containing less Ca exhibit smaller decreases in the calculated concentrations of the elements.

## RESULTS

### Quartz-hosted fluid inclusions

Results of the LA-ICP-MS analyses of secondary, quartz-hosted L-V and L-V-H inclusions are summarized in Table 4. Sodium and K were detected in all quartz-hosted inclusions. Strontium was detected in the majority, Ca and Ba were detected in approximately half, and Y, Nb, Ce, Sm, Th and U were detected in two or three of these inclusions, typically in concentrations less than 10 µg/g. Beryllium, Zr and Ho were not detected in quartz-hosted inclusions, although only four analyses included Be and only five included Zr.

The common occurrence of Na, K, Ca, Sr and Ba in quartz-hosted inclusions makes these elements useful in illustrating the different compositional groups and trends within these inclusions. Approximately half of the quartz-hosted L-V and L-V-H inclusions in this study do not contain detectable concentrations of Ca. Therefore, quartz-hosted inclusions can be divided into two compositional subgroups based on the presence or absence of Ca (Table 4).

Calcium-bearing quartz-hosted inclusions have Ca concentrations ranging from 51,100 to 101,000 µg/g and K concentrations ranging from 395 to 2,270 µg/g (Fig. 6A). In inclusions that contain detectable amounts of both elements, the concentration of K appears to increase with increasing Ca concentration (Fig. 6A). In contrast, Ca-free (below detection) quartz-hosted inclusions have K concentrations ranging from 12 to 5,110 µg/g (Fig. 6A). These relationships allow us to define three types of fluid (Fig. 6A): F1 comprise Ca-free, low-K inclusions, F2 comprise Ca-bearing inclusions, and F3 comprise Ca-free, high-K inclusions.

The majority of quartz-hosted inclusions have Na concentrations between 85,000 and 120,000 µg/g and K concentrations between 500 and 2,500 µg/g (Fig. 6B). Some quartz-hosted L-V-H inclusions, however, have lower Na, and one L-V and one L-V-H inclusion have higher K concentrations than the other quartz-hosted inclusions (Fig. 6B). Inclusions of the F2 type of fluid

show a decrease in Na with increasing K and Ca (Figs. 6B, C). Calcium-bearing, quartz-hosted L-V and L-V-H inclusions (F2) exhibit a continuum in composition between L-V-H inclusions, which have Ca concentrations up to approximately 75,000  $\mu\text{g/g}$  and Na concentrations as low as approximately 50,000  $\mu\text{g/g}$ , to predominantly L-V inclusions, which have Na concentrations up to approximately 102,000  $\mu\text{g/g}$  and Ca concentrations as low as approximately 6,200  $\mu\text{g/g}$  (Fig. 6C). Calcium-bearing L-V inclusions have a restricted range of Na concentrations (99,400 to 101,300  $\mu\text{g/g}$ ) and generally lower concentrations of Ca relative to Ca-bearing L-V-H inclusions, suggesting that the continuum of compositions exhibited by these inclusions

may comprise two separate compositional trends: 1) relatively constant Na and variable Ca, and 2) high Ca and low Na to low Ca and high Na.

Quartz-hosted, F2 inclusions also exhibit a positive correlation between the concentrations of Ca and Sr (Fig. 7A) and Ca and Ba (Fig. 7B). In the absence of data on Ca for fluorite-hosted fluid inclusions, the positive correlation among these elements, particularly Sr, is useful in inferring whether quartz-hosted and fluorite-hosted fluid inclusions have similar compositions. A comparison of quartz- and fluorite-hosted fluid inclusions is discussed below.

Although fluid F1 is represented predominantly by L-V inclusions and fluid F2 is represented predominantly by L-V-H inclusions, it is significant that both L-V and L-V-H inclusions occur within each type of fluid. These data suggest that the absence of halite is not reflective of compositional differences, but rather is due to the failure of halite to nucleate in some fluid inclusions.

TABLE 4. SUMMARY OF COMPOSITIONAL DATA, QUARTZ-HOSTED FLUID INCLUSIONS, OREGON No. 3 GRANITIC PEGMATITE, SOUTH PLATTE DISTRICT, COLORADO

Element	Range (ppm)	Average (ppm)	Number (n)
<b>All inclusions</b>			
Be	--	n.d.	4
Na	51,111 to 117,000	95,994	27
K	12 to 5,110	1,617	27
Ca	n.d. to 80,630	19,450	27
Sr	n.d. to 1,303	256	27
Y	n.d. to 169	6	27
Zr	--	n.d.	4
Nb	n.d. to 17	1	27
Ba	n.d. to 1,119	146	23
Ce	n.d. to 86	3	27
Sm	n.d. to 5	n.d.	17
Ho	--	n.d.	10
Th	n.d. to 6	0	27
U	n.d. to 96	4	27
<b>Ca-bearing inclusions</b>			
Be	--	n.d.	1
Na	51,111 to 101,279	80,477	11
K	395 to 2,271	1,507	11
Ca	6,201 to 80,630	47,741	11
Sr	57 to 1,303	608	11
Y	0 to 5	n.d.	11
Zr	--	n.d.	2
Nb	0 to 3	n.d.	11
Ba	5 to 1,119	364	9
Ce	0 to 5	1	11
Sm	0 to 5	1	7
Ho	--	n.d.	4
Th	0 to 4	n.d.	11
U	0 to 11	1	11
<b>Ca-free inclusions</b>			
Be	--	n.d.	3
Na	91,300 to 117,000	106,663	16
K	12 to 5,110	1,692	16
Ca	--	n.d.	16
Sr	0 to 66	14	16
Y	0 to 169	11	16
Zr	--	n.d.	2
Nb	0 to 17	1	16
Ba	0 to 69	7	14
Ce	0 to 96	5	16
Sm	--	n.d.	10
Ho	--	n.d.	6
Th	0 to 6	n.d.	16
U	0 to 96	6	16

#### FLUORITE-HOSTED FLUID INCLUSIONS

The LA-ICP-MS analyses of L-V inclusions hosted in purple, white and colorless fluorite, and L-V-H inclusions hosted in white fluorite, are summarized in Tables 5 and 6, respectively. Sodium and K were detected in all fluorite-hosted inclusions (Fig. 8). Strontium and Ba were detected in the majority, and Y, Nb, Ce, Sm, Th and U were detected in only a few inclusions. As was the case for quartz-hosted inclusions, Be, Zr and Ho were not detected in fluorite-hosted inclusions, although only a limited number of analyses were performed for Be and Zr.

Fluorite-hosted L-V inclusions have Na concentrations ranging from 41,300 to 48,400  $\mu\text{g/g}$ , K concentrations ranging from below detection to 851  $\mu\text{g/g}$ , Sr concentrations ranging from below detection to 652  $\mu\text{g/g}$ , and Ba concentrations ranging from below detection to 11  $\mu\text{g/g}$ . The two fluorite-hosted L-V-H inclusions have a Na concentration of 95,200  $\mu\text{g/g}$  [both inclusions had the same  $T_m(\text{NaCl})$ ], K concentrations of 1,210 and 1,590  $\mu\text{g/g}$ , Sr concentrations of 546 and 786  $\mu\text{g/g}$ , and Ba concentrations either below detection or 353  $\mu\text{g/g}$ .

The  $T_m$  (ice) data indicate that all L-V inclusions hosted in purple, white and colorless fluorite have comparable salinities. These data, combined with the results of LA-ICP-MS analyses, indicate that Na, K, Sr and Ba concentrations in L-V inclusions hosted in white, colorless and purple fluorite are all similar, but that in purple fluorite, L-V inclusions have higher concentrations of Ce, Sm, Th and U. As the sequence of fluorite crystallization is purple, white and then colorless, there was thus a temporal evolution in fluid composition toward lower Ce, Sm, Th and U concentrations at relatively constant salinity. Homogenization temperatures of L-V inclusions in the three types of fluorite are es-

essentially the same (80 to 115°C), indicating that the evolution in fluid composition occurred isothermally.

*Comparison of quartz- and fluorite-hosted fluid inclusions*

Sodium, K, Ca, Sr and Ba concentrations can be used to illustrate the relationships between the various types of quartz- and fluorite-hosted inclusions (Figs. 8, 9, 10). In order to plot the fluorite-hosted inclusions on Figure 9, we have assumed that the fluorite-hosted inclusions contain little or no Ca. This is a reasonable assumption based on the low solubility of fluorite at the salinities represented by the fluorite-hosted inclusions (Richardson & Holland 1979). The compositions of fluorite-hosted inclusions have not been corrected for

the effect of Ca on  $Na_{MT}$ , as discussed above; if the correction were performed, and assuming that there is significant Ca in the fluorite-hosted inclusions, the concentration of Na would decrease, and concentrations of other elements (K, Sr, and Ba) would decrease proportionally. Correcting  $Na_{MT}$  in the data in Figure 9 would cause the fluorite-hosted L-V and L-V-H inclusions to move from the Na-K binary join toward the Ca apex and away from the Na apex. Because K, Ba and Sr would change proportionally, the effect on Figure 10 would be negligible. Understanding the potential effect that the Ca correction would have on  $Na_{MT}$  enables direct comparison of corrected data from quartz-hosted fluid inclusions with uncorrected data from fluorite-hosted fluid inclusions.

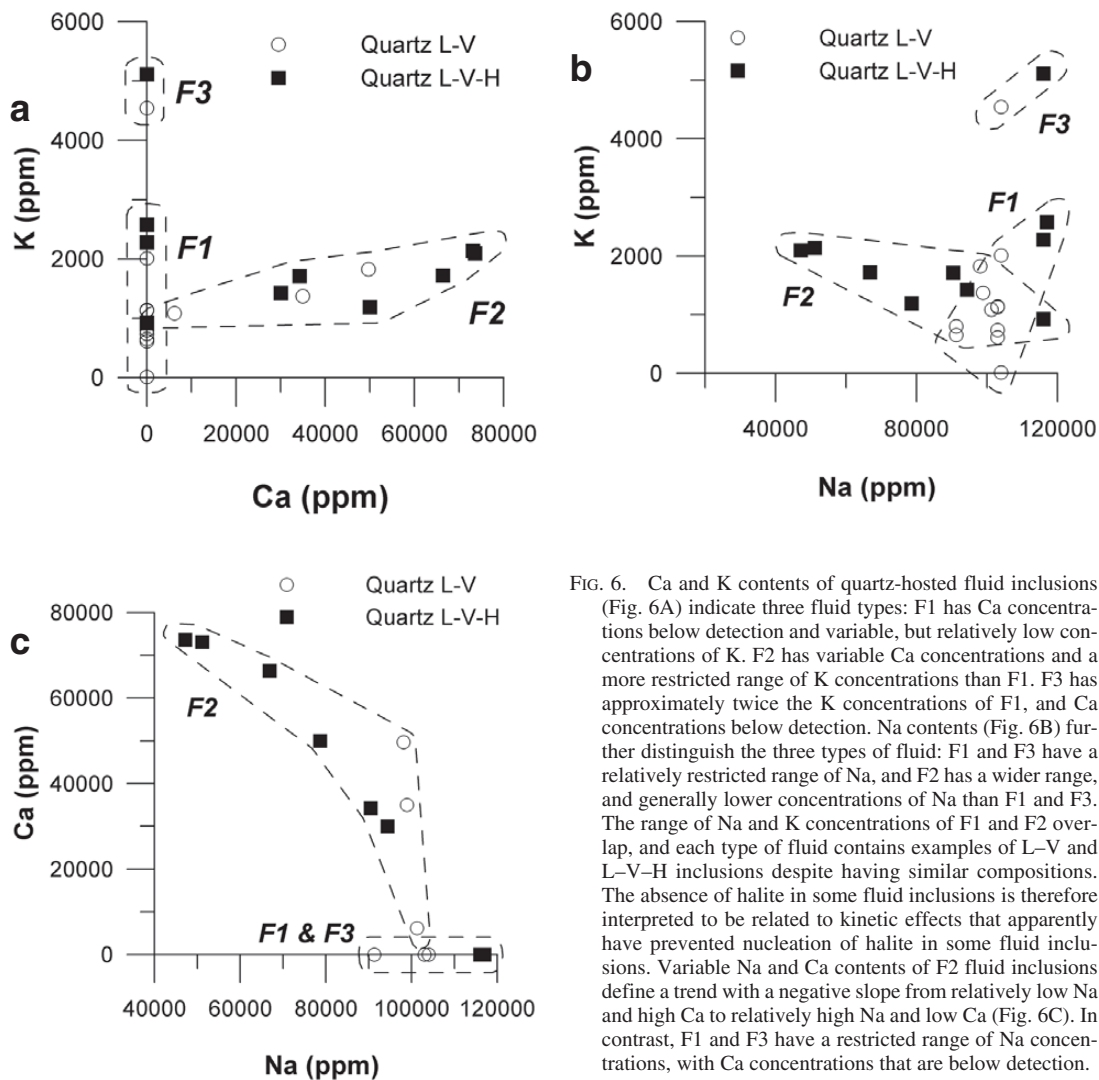


FIG. 6. Ca and K contents of quartz-hosted fluid inclusions (Fig. 6A) indicate three fluid types: F1 has Ca concentrations below detection and variable, but relatively low concentrations of K. F2 has variable Ca concentrations and a more restricted range of K concentrations than F1. F3 has approximately twice the K concentrations of F1, and Ca concentrations below detection. Na contents (Fig. 6B) further distinguish the three types of fluid: F1 and F3 have a relatively restricted range of Na, and F2 has a wider range, and generally lower concentrations of Na than F1 and F3. The range of Na and K concentrations of F1 and F2 overlap, and each type of fluid contains examples of L-V and L-V-H inclusions despite having similar compositions. The absence of halite in some fluid inclusions is therefore interpreted to be related to kinetic effects that apparently have prevented nucleation of halite in some fluid inclusions. Variable Na and Ca contents of F2 fluid inclusions define a trend with a negative slope from relatively low Na and high Ca to relatively high Na and low Ca (Fig. 6C). In contrast, F1 and F3 have a restricted range of Na concentrations, with Ca concentrations that are below detection.

Fluorite-hosted L-V inclusions have lower concentrations of Na and K than fluorite-hosted L-V-H or quartz-hosted inclusions. Fluorite-hosted L-V-H inclusions have compositions similar to quartz-hosted Ca-free inclusions (F1) (Figs. 8, 9). If the  $Na_{MT}$  of the fluorite-hosted L-V inclusions were corrected, the inclusions would plot in an area of the Na-K-Ca diagram that, with the exception of one quartz-hosted L-V inclusion, is devoid of other fluid inclusions (arrows, Fig. 9). However, if the fluorite-hosted L-V-H inclusions were Ca-bearing and  $Na_{MT}$  were corrected, the inclusions would potentially plot in an area of the Na-K-Ca diagram where quartz-hosted Ca-bearing inclusions plot. Fluorite-hosted L-V-H inclusions thus would have similar major-element compositions to either quartz-hosted Ca-bearing (F2) or Ca-free inclusions (F1).

Fluorite-hosted L-V inclusions have proportionally higher concentrations of Sr and lower concentrations of K and Ba than fluorite-hosted L-V-H and quartz-hosted inclusions (Fig. 10). These inclusions plot near the Sr apex of the Sr-K-Ba diagram (Fig. 10) because K and Ba concentrations are relatively low and not because Sr concentrations are particularly high. Furthermore, correction of  $Na_{MT}$  would have a negligible effect on the element relationships in Figure 10. One of the fluorite-hosted L-V-H inclusions plots with the quartz-hosted Ca-bearing inclusions (F2), and the other plots on the K-Sr binary join because Ba was not detected in this inclusion. These two inclusions plot together on Fig-

ure 8 along with quartz-hosted L-V-H inclusions, suggesting that both inclusion assemblages represent the same type of fluid.

White fluorite-hosted L-V-H inclusions have higher Na, K, Sr and Ba concentrations than fluorite-hosted L-V inclusions (F4). White fluorite-hosted L-V-H inclusions have similar K:Na, Sr:Na and Ba:Na ratios to quartz-hosted Ca-bearing inclusions (F2) (Fig. 11). Quartz-hosted Ca-free inclusions (F1 and F3) have variable K:Na and generally lower Sr:Na and Ba:Na ratios than quartz-hosted Ca-bearing (F2) and white fluorite-hosted L-V-H inclusions. The similarity between the element concentrations and ratios of white fluorite-hosted L-V-H and quartz-hosted Ca-bearing inclusions (Figs. 8, 11) suggests that these two fluid-inclusion assemblages represent that same type of fluid (F2).

We conclude that: 1) fluorite-hosted L-V inclusions have a different composition from quartz-hosted inclusions and fluorite-hosted L-V-H inclusions and represent a different type of fluid (F4), and 2) fluorite-hosted L-V-H inclusions have compositions and element ratios that are similar to quartz-hosted Ca-bearing inclusions and likely correspond to the same type of fluid (F2). Furthermore, we infer from these similarities that white-fluorite-hosted L-V-H inclusions may also be Ca-bearing. The average Sr:Ca ratio of quartz-hosted, Ca-bearing inclusions is 0.013. If the average Sr:Ca ratio of quartz-hosted, Ca-bearing fluid inclusions and the Sr concentration of white fluorite-hosted L-V-H inclusions are used to calculate a hypothetical concentration

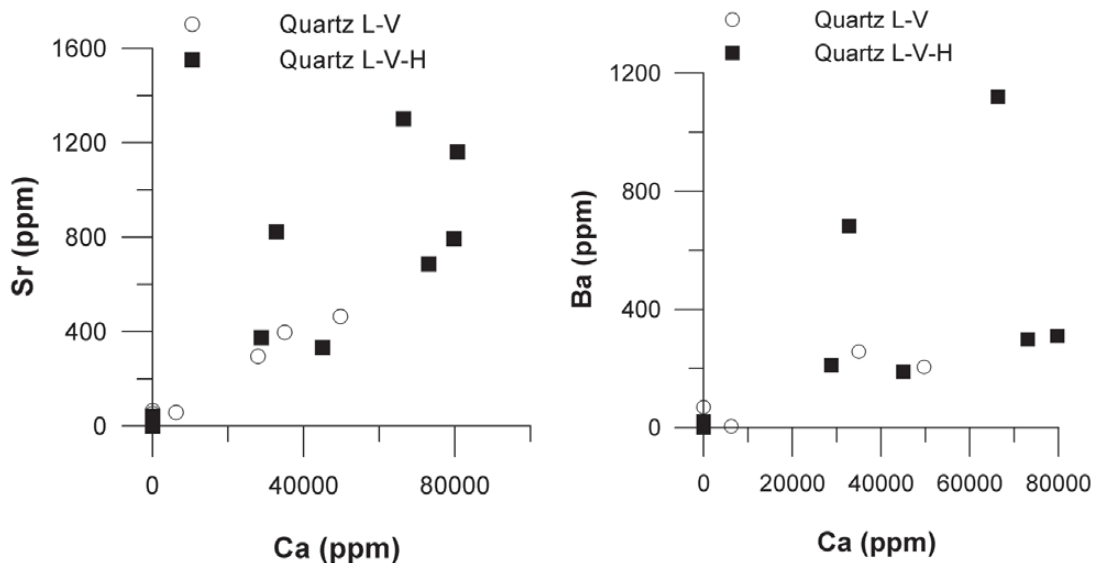


FIG. 7. Strontium (Fig. 7A) and Ba (Fig. 7B) concentrations exhibit positive relationships with Ca concentrations in Ca-bearing quartz-hosted fluid inclusions (F2). In contrast, F1 and F3, which have Ca concentrations below detection, plot as a cluster near the origin.

of Ca, the white-fluorite-hosted inclusions would contain approximately 51,200  $\mu\text{g/g}$  Ca. It is possible that Ca concentrations in the fluorite-hosted fluids were affected by equilibration with, or precipitation of fluorite; the observation that Sr and Ba contents are similar to the quartz-hosted inclusions suggests that this is not the case, however, as those elements are readily incorporated into fluorite (Gagnon *et al.* 2003b). The inference that white-fluorite-hosted L–V–H inclusions are Ca-bearing and are the same type of fluid as quartz-hosted Ca-bearing inclusions has implications for the origin and timing of the hydrothermal fluid events, which are discussed below.

TABLE 5. SUMMARY OF COMPOSITIONAL DATA, FLUORITE-HOSTED L–V FLUID INCLUSIONS, OREGON No. 3 GRANITIC PEGMATITE, SOUTH PLATTE DISTRICT, COLORADO

Element	Range (ppm)	Average (ppm)	Number (n)
<b>Purple fluorite</b>			
Be	--	--	--
Na	41,300 to 43,200	42,250	2
K	286 to 375	331	2
Ca	--	--	--
Sr	136 to 240	188	2
Y	n.d. to 1,590	795	2
Zr	--	--	--
Nb	n.d. to 1	1	2
Ba	n.d. to 8	4	2
Ce	152 to 173	163	2
Sm	61 to 105	83	2
Ho	--	--	--
Th	271 to 1,930	1,101	2
U	5 to 13	9	2
<b>White fluorite</b>			
Be	--	n.d.	3
Na	42,100 to 48,400	44,700	5
K	n.d. to 851	231	5
Ca	--	--	--
Sr	n.d. to 652	199	5
Y	n.d. to 54	11	5
Zr	--	n.d.	3
Nb	--	n.d.	5
Ba	3 to 7	5	2
Ce	n.d. to 10	2	5
Sm	n.d. to 4	1	3
Ho	--	n.d.	2
Th	n.d. to 12	6	5
U	n.d. to 1	n.d.	5
<b>Colorless fluorite</b>			
Be	--	--	--
Na	--	42,900	3
K	123 to 150	139	3
Ca	--	--	--
Sr	207 to 313	262	3
Y	--	n.d.	3
Zr	--	--	--
Nb	--	n.d.	3
Ba	4 to 11	8	3
Ce	n.d. to 420	140	3
Sm	--	--	--
Ho	--	n.d.	2
Th	n.d. to 26	9	3
U	--	n.d.	3

## DISCUSSION

### Sources of fluid

Microthermometric and LA–ICP–MS analyses indicate that at least four compositionally distinct types of

TABLE 6. SUMMARY OF COMPOSITIONAL DATA, WHITE-FLUORITE-HOSTED L–V–H FLUID INCLUSIONS, OREGON No. 3 GRANITIC PEGMATITE, SOUTH PLATTE DISTRICT, COLORADO

Element	Range (ppm)	Average (ppm)	Number (n)
Be	--	--	--
Na	--	95,200	2
K	1,210 to 1,590	1,400	2
Ca	--	--	--
Sr	546 to 786	666	2
Y	--	n.d.	2
Zr	--	--	--
Nb	--	n.d.	2
Ba	n.d. to 353	177	2
Ce	--	n.d.	2
Sm	--	--	--
Ho	--	n.d.	2
Th	--	n.d.	2
U	--	n.d.	2

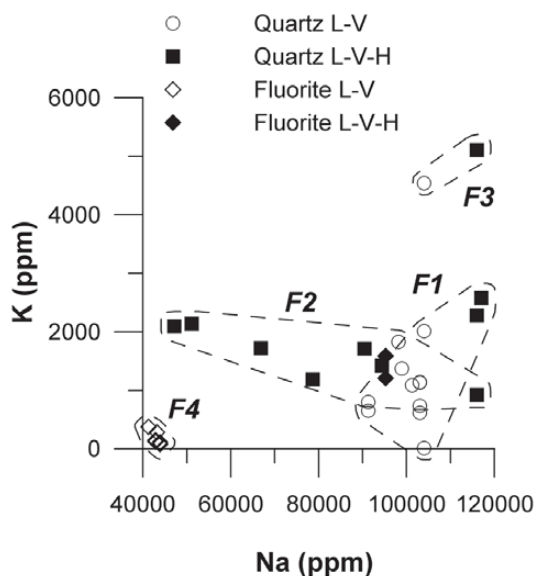


FIG. 8. Sodium and K concentrations of white fluorite-hosted L–V–H inclusions are similar to those of quartz-hosted Ca-bearing L–V–H inclusions (F2). L–V inclusions hosted by purple, white, and colorless fluorite, however, have lower Na and K concentrations than all quartz-hosted L–V and L–V–H inclusions (F1, F2 and F3) and white-fluorite-hosted L–V–H inclusions (F2?), indicating that a different fluid (F4) was responsible for the hydrothermal fluorite–REE mineralization.

hydrothermal fluid (F1 through F4) occur within the Oregon No. 3 pegmatite. Only F4, which is a Na–K–Ca–Sr–Ba-bearing and relatively low-salinity (9 to 12 wt.% NaCl equiv.) fluid, seems to have caused the secondary hydrothermal fluorite–REE mineralization. Potential sources of hydrothermal fluids in the Oregon No. 3 pegmatite are fluids derived internally, late in the crystallization history of the granitic pegmatite, and fluid(s) derived from outside the pegmatite, either from the Pikes Peak granite or the enclosing country-rocks. The pegmatite is presently situated approximately 5 km from the nearest country-rocks. Simmons & Heinrich (1980) interpreted the occurrence of country-rock xenoliths in granite proximal to the pegmatite to indicate emplacement of the pegmatite near the top of the granite pluton, however. Although it is possible that fluid from the country rocks could have been involved, migration of any formation waters through the granite would have resulted in compositional modification as a result of varying degrees of equilibration with the granite. Furthermore, extensive, secondary fluorite–REE mineralization selectively replaces the upper parts of the

pegmatites, particularly the top of the quartz core and upper core-margin zone of the Oregon No. 3 pegmatite, suggesting that there is an intimate link between the secondary mineralization and pegmatite crystallization (Simmons & Heinrich 1980). Data on fluid and mineral compositions and modeling of the fluid–rock reaction (discussed below) indicate that the introduction of elements (*e.g.*, Ca) into the pegmatite from the country rocks, as has occurred in some other cases of hydrothermal REE mineralization (*e.g.*, Salvi & Williams-Jones 1990, Williams-Jones *et al.* 2000), was not necessary to form the hydrothermal fluorite–REE mineralization in the Oregon No. 3 pegmatite. Therefore, the most plausible sources of the hydrothermal fluids are the pegmatite itself or a late phase of the Pikes Peak granite.

The hydrothermal fluids responsible for the fluorite–REE mineralization (F4), whether internally or externally derived, were out of chemical equilibrium with wall-zone K-feldspar and magmatic core-margin fluorite at the P–T–X conditions of formation of the fluorite–REE mineralization, as evidenced by the extensive albitization associated with fluorite–REE mineraliza-

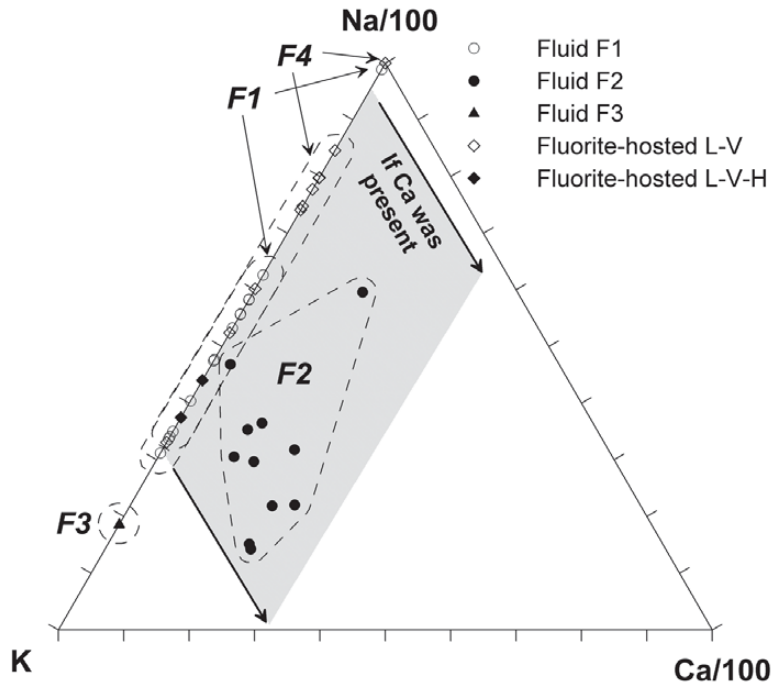


FIG. 9. Na–K–Ca relationships of quartz- and fluorite-hosted fluid inclusions. Concentrations of Ca that are below detection in some quartz-hosted inclusions (F1 and F3), and the inability to quantify Ca concentrations in fluorite-hosted inclusions (F4), cause these inclusions to plot along the Na–K binary join. Correction of some compositions of fluorite-hosted fluid inclusions for the presence of Ca, however, would cause them to plot with F2 inclusions, suggesting that these inclusions may have the same composition as quartz-hosted F2.

tion, and by the replacement of primary, magmatic green fluorite by purple, white and colorless fluorite (Simmons & Heinrich 1980). If the source of fluid F4 was the Pikes Peak granite, the fluid represented by the fluorite-hosted L-V inclusions would be in chemical equilibrium with the granite at the prevailing condition in the granite. The following questions arise: 1) would such a fluid, upon interaction with the pegmatite wall and core-margin zones, cause albitization and dissolution of fluorite, and 2) how would the composition of such a fluid compare to the observed fluid-inclusion compositions? In order to address these questions, we have used the HCh software package (Shvarov & Bastrakov 1999) and the SUPCRT database (Johnson *et al.* 1992), modified by Shock (1998), to react a hypothetical fluid in chemical equilibrium with the Pikes Peak granite with the pegmatite wall-zone to determine whether the fluid would cause albitization. A hypothetical composition was determined for aqueous brine in equilibrium with an average composition of the Pikes Peak granite, calculated using data presented in Hutchinson (1960) and Smith *et al.* (1999). The aqueous brine was then reacted with the pegmatite wall-zone, the composition of which was calculated by averaging 13 compositions reported in Simmons *et al.* (1987). Fluid-rock reaction was con-

ducted at a temperature and pressure of 200°C and 2000 bars, respectively, which are reasonable estimates based on pressure-corrected temperatures obtained from our microthermometric analysis and the pressure estimates of Simmons *et al.* (1987), which are based on phase equilibria in the systems Q-Ab-Or-An-H<sub>2</sub>O (Simmons & Heinrich 1980) and Q-Ab-Or-H<sub>2</sub>O (Barker *et al.* 1975).

Fluid-rock interaction was modeled by reacting 100 grams of pegmatite wall-zone with incrementally increasing volumes of fluid. The starting fluid:rock ratio was arbitrarily set at 0.03, which is considered to be a low but geologically reasonable value. The fluid:rock ratio was incrementally increased until the final ratio was between approximately 3 and 8. At the start of the model, the equilibrium speciation of the fluid was calculated from the initial composition of the fluid and log K values for all plausible reactions involving the different aqueous species that could theoretically form. After each incremental addition of fluid, the rock and fluid were brought to chemical equilibrium by considering all possible reactions governing speciation, mineral deposition, and mineral dissolution. The compositions of rock and fluid were then recomputed, and the fluid respesiated.

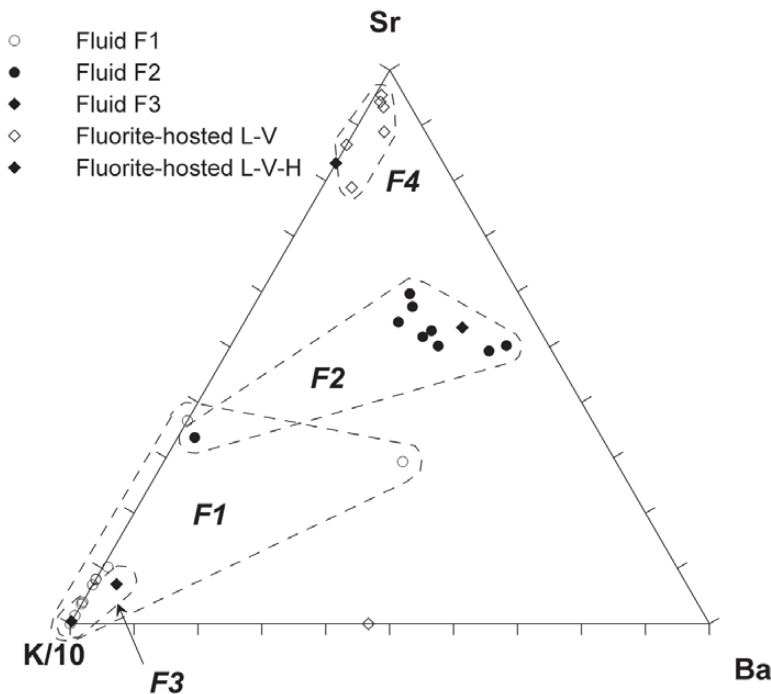


FIG. 10. Sr-K-Ba relationships of quartz- and fluorite-hosted fluid inclusions. Fluorite-hosted L-V inclusions plot near the Sr apex, indicating that these inclusions have a composition that is unique with respect to other fluorite- and quartz-hosted inclusions.

The average concentrations of Na, K, Ca, Sr and Ba in type F1, F2, F3 and F4 fluids and the hypothetical fluid in compositional equilibrium with the Pikes Peak granite are presented in Table 7. The results of the modeling are presented graphically in Figure 12. The hypothetical, granite-equilibrated fluid has a lower concentration of Na relative to type-F1 through type-F4 fluids, a K content that lies within the range of that for the F1 through F4 fluids, and a lower concentration of Ca than type F2 fluid, the only other Ca-bearing fluid identified (Table 8). Reaction of the granite-equilibrated fluid with the wall zone results in alteration of the rock to K-feldspar (Fig. 12A). At fluid:rock ratios greater than approximately 0.1, the microcline perthite begins to lose albite in favor of microcline, and at a ratio of approximately 3, microcline perthite is replaced entirely by microcline. Therefore, a fluid that had equilibrated with the Pikes Peak granite would have had a composition different from type F1 through F4 fluids, could not have caused the observed albitization of the wall zone and, by itself, could not have been responsible for the hydrothermal fluorite-REE mineralization. Therefore, it appears most likely that a hydrothermal fluid derived within the pegmatite was responsible for the secondary fluorite-REE mineralization.

The lack of Ca data for fluid F4 makes it difficult to quantitatively model interaction of this fluid with the wall zone and to test whether or not it would cause albitization. Although the fluids represented by the quartz-hosted fluid inclusions do not appear to have been directly associated with the fluorite-REE mineralization, their origins are of interest in constraining potential sources of fluids within the pegmatite. Therefore, the average composition of each of the three quartz-hosted fluids (F1, F2 and F3) was reacted with the wall zone to determine whether the fluids could cause albitization. Modeling was conducted under the same P-T conditions as for the reaction between granite-derived fluid and wall zone.

The results of the modeling are presented graphically in Figure 12 (B, C, D) and indicate that reaction of any

of the three quartz-hosted fluid inclusion compositions with pegmatite wall-zone would result in albitization. At water:rock ratios greater than approximately 0.1, microcline is ion-exchanged to albite and at ratios ranging from 4 (Fig. 12D) to 8 (Fig. 12B), microcline is replaced entirely by albite, a reaction that causes secondary porosity. The dissimilarity between the results of modeling involving hypothetical granite-equilibrated and quartz-hosted fluid compositions and the wall zone indicates that the quartz-hosted fluids, although apparently not directly involved in the fluorite-REE min-

TABLE 7. COMPARISON OF FLUID INCLUSION AND MODELED COMPOSITIONS OF FLUID, OREGON No. 3 GRANITIC PEGMATITE AND PIKES PEAK GRANITE, SOUTH PLATTE DISTRICT, COLORADO

	Quartz F1	Quartz F2	Fluorite F2	Quartz F3	Fluorite F4	Pikes Peak gr.
Na	106,000	112,000	95,200	110,000	43,700	27,000
K	1,250	2,415	1,400	4,800	224	2,600
Ca	n.d.	81,000	n.d.	n.d.	--	6,560
Sr	13	1,000	670	22	220	--
Ba	6	600	180	11	6	--

Footnotes: All concentrations reported as ppm (mg/g). -- : indicates that sample was not analyzed for this element. n.d.: indicates that the concentration of the element is below the limit of detection.

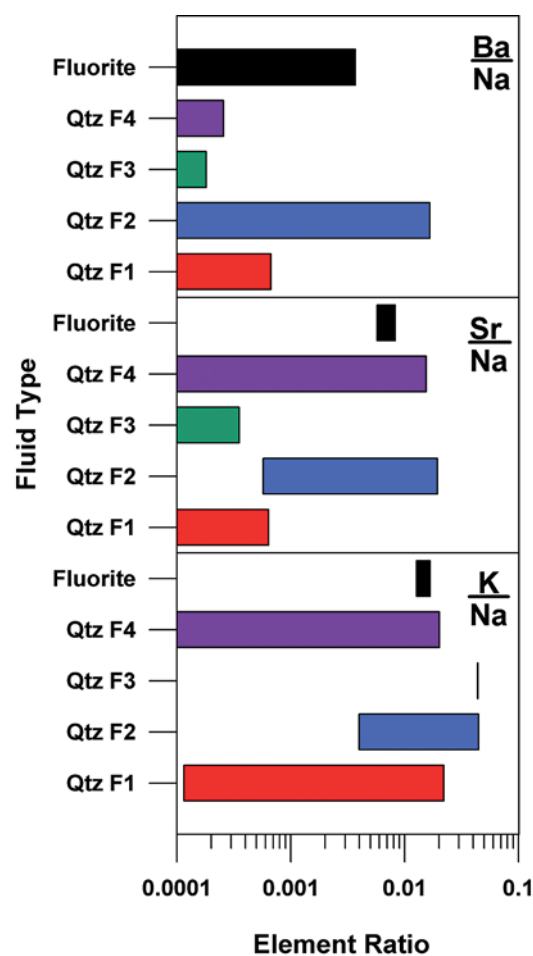


FIG. 11. Element ratios by fluid type. Fluorite-hosted L-V-H inclusions have K:Na and Sr:Na ratios that plot at approximately the center of the range of K:Na and Sr:Na ratios exhibited by Ca-bearing quartz-hosted inclusions (F2). The Ba:Na ratios of these fluorite-hosted inclusions also overlap with the ratios of the quartz-hosted inclusions. These relationships indicate that these two assemblages of fluid inclusions represent the same type of fluid.

eralization, were derived internally from the pegmatites and could also have caused albitization of the wall zone.

The modeling of the fluid–rock reaction indicates that the most significant factor controlling whether conversion of perthite to albite or to microcline occurs in the wall zone is the K:Na ratio of the hydrothermal fluid. The hypothetical fluid in compositional equilibrium with the Pikes Peak granite has a K:Na ratio of approximately 0.1. In contrast, compositions of quartz-hosted fluid inclusions have K:Na ratios ranging from 0.01 to 0.03. Fluorite-hosted fluid inclusions have even lower K:Na ratios (approximately 0.005), indicating that if this fluid composition had reacted with the wall zone, albitization would likely occur at even lower fluid:rock ratios than for a fluid such as that trapped in the quartz-hosted fluid inclusions. The results of the modeling of the fluid–rock reaction are consistent with models in which albitization, and by association the fluorite–REE mineralization, was caused by fluids derived within the pegmatite.

#### *Fluid relationships*

LA–ICP–MS analyses indicate that four types of fluid occur within the Oregon No. 3 pegmatite. Modeling of the fluid–rock reaction indicates that these fluids were likely derived internally, within the pegmatite. If so, what may have caused the compositional variations within F1 and F2 (Figs. 6, 7, 8) and what are the possible relationships among F1, F2, F3 and F4 (Figs. 8, 9, 10)? It is implied from the overlap in the compositions of F1 and F2 fluid inclusions and the trends in the data (Figs. 6, 7) that either two different processes caused evolution of a single fluid (F1) into two different compositions (F2 and F3), or two different fluids (F2 and F3) evolved toward a single composition of fluid (F1). Compositional trends between the fluid mainly responsible for the fluorite–REE mineralization (F4) and the other potentially related fluids (F1 through F3) are not readily apparent (Figs. 9, 10).

Processes known to have occurred within the pegmatite at the temperature of mineralization that have the potential to cause systematic variations in fluid composition are: 1) dissolution of the green, magmatic fluorite, 2) precipitation of purple, white and colorless fluorite, and 3) reaction of fluids with the wall zone (albitization). Although other processes may have been involved (*e.g.*, precipitation of other minerals, reaction with another rock-type, or introduction of an externally derived fluid other than one in chemical equilibrium with the Pikes Peak granite), the observed variations in fluid compositions are evaluated below to determine whether the trends can be explained in the context of the three processes that are known to have occurred within the pegmatite. Data presented by Gagnon *et al.* (2003b) indicate that the green fluorite has higher average concentrations of Ca and Sr and lower concentrations of Na, K and Ba than F1. Therefore, dissolution of

green fluorite by F1 would lead to greater relative increases in the concentrations of Ca and Sr in the fluid than Na, K and Ba. Although F1 does exhibit a trend of increasing Na and K that could be attributed to dissolution of fluorite (Fig. 13A), a concomitant change in Ca concentrations is not evident (Fig. 13B). Similarly, with the exception of K, compositional variation within F2 could be explained through dissolution of primary green fluorite or, alternatively, secondary hydrothermal purple, white or colorless fluorite (Fig. 13C). Compositional variation within and between Ca-free fluids (F1 and F3) cannot be entirely explained by reaction of either fluid with fluorite.

Data from Gagnon *et al.* (2003b) on the chemical composition of purple, white and colorless fluorite and on the composition of primary fluid inclusions in fluorite from this study were used to calculate mineral–fluid partition coefficients ( $K_d$ ) for Na, K, Sr and Ba (Table 8). Because these elements are incorporated into fluorite, fluorite precipitation will deplete the fluid in all these components. The partition coefficients, however, indicate that the precipitation of purple fluorite would cause greater depletion in Ca and Ba in the fluid than in Na, K and Sr, the precipitation of white fluorite would cause greater depletion in Ca, K and Ba in the fluid than in Na and Sr, and the precipitation of colorless fluorite would cause greater depletion in Ca in the fluid than in Na, K, Sr and Ba. The positive trend exhibited by Ca and K concentrations in F2 (Fig. 13C) is consistent with fluorite deposition. The negative trends in the Na and Ca concentrations (Fig. 13B) and Na and K concentrations of F2 (Fig. 13A), however, cannot be explained by fluorite precipitation. The lack of a trend in Ca concentrations due to concentrations of Ca below detection, implies that progressive precipitation of fluorite was not responsible for the compositional variation exhibited by F1 and cannot explain potential relationships between F1 and F3 (Fig. 13). The possibility exists, however, that F1 and F3 represent residual fluids that have been depleted in Ca and other elements as a result of fluorite precipitation. The  $K_d$  values indicate that fluorite deposition would result in a fluid with lower Na, K, Ca, Sr and Ba than the starting composition of the fluid. Primary fluorite-hosted fluid inclusions (F4), however, have lower salinities than type F1 and F3 fluids. Precipitation of fluorite from such fluids, although resulting in lower concentrations of cations, would not affect the bulk salinity of the hydrothermal fluid owing to the anhydrous nature and the lack of chlorine consumption during progressive precipitation of fluorite. Therefore, the differences in the compositions of F1 and F3 relative to F4 cannot be explained by precipitation of purple, white or colorless fluorite.

Progressive dissolution of pre-existing primary green or secondary purple, white or colorless fluorite is expected to result in variations in fluid composition similar to those likely to occur during fluorite precipitation. The direction of the trends, however, would be toward

higher concentrations of Na, K, Ca, Sr and Ba in the fluid with increasing amounts of fluorite dissolution rather than the lower concentrations that would result from fluorite precipitation. The negative trend exhibited by Na and Ca concentrations for type F2 fluid (Fig. 13B) and the lack of detectable concentrations of Ca in types F1 and F3 fluids are inconsistent with fluorite dissolution.

Interaction of the fluids represented by quartz-hosted inclusions (F1, F2 and F3) with the pegmatite wall-zone, in addition to causing albitization, causes a compositional evolution of the coexisting fluid. Progressive reaction of hydrothermal fluid with the wall zone causes an increase in the concentrations of Ca and K in the fluid due to replacement of microcline perthite by albite. Significant increases in Ca and K concentrations in the fluid occur at relatively low fluid:rock ratios (less than 0.1). In contrast, the Na concentration in the fluid is reduced owing to the precipitation of albite. Compositional trends observed in F2 are characterized by increasing K (Fig. 13B) and Ca (Fig. 13A) and decreasing Na or in F1 by increasing K at relatively constant Na (Fig. 13A) and lacking Ca (Figs. 13B, C). Therefore, the compositional variation exhibited by F2 can be explained through progressive reaction of fluid(s) with the pegmatite wall-zone. Compositional variation within F1, or the potential relationship between F1 and F3, cannot be explained by the same process.

In summary, some of the compositional variation in the fluids found as inclusions within the quartz core (F1, F2 and F3) can be explained by processes related to the secondary hydrothermal fluorite-REE mineralization. These fluid inclusions are, however, secondary in origin, different in composition from the primary fluid inclusions hosted by fluorite (F4) and, with the exception of L-V-H inclusions in white fluorite (F2), whose provenance is equivocal, have not been observed as primary fluid inclusions within fluorite. Therefore, the interpretation of the variations in the compositions of quartz-hosted fluid inclusions in the context of the fluorite-REE mineralization must be regarded as speculative in nature.

#### *Timing and cause of fluorite-REE mineralization*

Four distinct types of fluid have been identified within the Oregon No. 3 pegmatite. Fluid F4, which was

responsible for the fluorite-REE mineralization, was not observed in the quartz core. Fluid compositions similar to those observed in secondary, quartz-hosted fluid inclusions (F1 and F3) were not observed in fluorite with the exception of L-V-H inclusions hosted by white fluorite (F2?). Therefore, the relative timing of the four fluid-circulation events is not readily apparent on the basis of fluid-inclusion petrography and compositions alone.

L-V-H fluid inclusions hosted by white fluorite have similar compositions to that of secondary, quartz-hosted Ca-bearing fluid inclusions (F2). The origin of white-fluorite-hosted L-V-H inclusions, however, is equivocal, and they have been identified as primary in origin only tentatively. If white-fluorite-hosted L-V-H inclusions are primary in origin, if they represent fluid type F2, and if the compositional variation in F2 is reflective of wall-zone albitization at 200°C, then precipitation of white fluorite occurred contemporaneously with wall-zone albitization. The alteration of the core-margin and wall zones, and the occurrence of vein and replacement-type fluorite-REE mineralization within the upper portions of the pegmatites (Simmons & Heinrich 1980), indicate that late-stage hydrothermal fluids derived within the pegmatite migrated from other portions of the pegmatite (likely underneath the mineralized zones) and reacted with the core-margin zone and wall zone.

The most likely causes of fluorite deposition from hydrothermal solutions are decreasing temperature, increasing pH, and mixing of solutions (Richardson & Holland 1979). Fluid-inclusion microthermometric analyses indicate that temperature was approximately constant over the period of time that the purple, white and colorless fluorite precipitated. Therefore, it is unlikely that decreasing temperature was the principal cause of fluorite precipitation. Modeling the reaction of pegmatite wall-zone with quartz-hosted fluids indicates that, with the exception of very high water:rock ratios (greater than 10:1), where a slight increase in pH (1 pH unit) was observed, fluid and wall-zone reaction occurs at approximately constant pH. The absence of hydration or dehydration reactions associated with the fluorite-REE mineralization, which would be indicative of considerable changes in pH of the hydrothermal fluid, support a relatively constant pH. Therefore, an increase in solution pH resulting from reaction with the pegmatite wall-zone does not appear to be the principal cause of fluorite precipitation. Modeling of the fluid-rock reaction and variation in the compositions of quartz-hosted fluid inclusions (F2) suggest that cation exchange involving Na for K and Ca occurred, which is most readily explained by the pegmatite wall-zone reaction. Potassium and Ca were liberated from the pegmatite wall-zone during albitization associated with fluorite-REE mineralization, and reacted with fluorine dissolved in the hydrothermal fluid and resulted in fluorite precipitation. Fluorite precipitation could occur even at low

TABLE 8. FLUID-FLUORITE PARTITION COEFFICIENTS

Element	Purple Fluorite	White Fluorite	Colorless Fluorite
Na	0.05	0.09	0.04
K	0.63	0.95	0.14
Sr	0.79	0.23	0.79
Ba	1.2	0.94	0.4

concentrations of Ca and F owing to the low solubility of fluorite (Richardson & Holland 1979). Therefore, the most likely cause of deposition of hydrothermal fluorite in albitized pegmatite wall-zone was cation exchange resulting from reaction of late fluids with the wall zone, which resulted in the addition to the fluid of cations liberated as a result of that albitization.

#### CONCLUSIONS

The following conclusions can be made based on the microthermometric and LA-ICP-MS analyses of quartz- and fluorite-hosted fluid inclusions and modeling of fluid-rock reaction associated with pegmatite-hosted fluorite-REE mineralization in the South Platte District, Colorado:

1) Quantitative LA-ICP-MS analysis of individual, relatively small (less than 15  $\mu\text{m}$ ) fluid inclusions in compositionally complex minerals such as fluorite is possible using a non-homogenized 266 nm Nd:YAG laser. Alternate opening strategies (traversed opening) are necessary to overcome difficulties associated with poor absorbance of laser energy and mineral cleavages. Subtraction of instrument and host-mineral backgrounds is inadequate to remove contributions to the fluid inclusion signal from the host mineral. The count rates obtained for elements potentially present within the fluid inclusions had to be ratioed against Ca count rates to quantitatively correct for the host-mineral contribution to the fluid-inclusion signal.

2) Four compositional types of fluid (F1, F2, F3 and F4) were identified in the Oregon No. 3 pegmatite; however, only one (F4) appears to have been directly involved in the secondary hydrothermal fluorite-REE mineralization. The fluids appear to have been derived internally with respect to the pegmatite, and fluorite precipitation appears to have occurred from F4 at relatively constant temperatures (81 to 114°C) and pH, largely as a result of mixing of Ca liberated from pegmatite wall-zone as a result of albitization with F-bearing hydrothermal fluid. The addition of elements such as Ca into the pegmatite through introduction of a fluid derived externally to the Pikes Peak granite was not

necessary to cause the hydrothermal fluorite-REE mineralization.

3) Compositional variation exhibited by one of the quartz-hosted fluids (F2), which does not appear to have

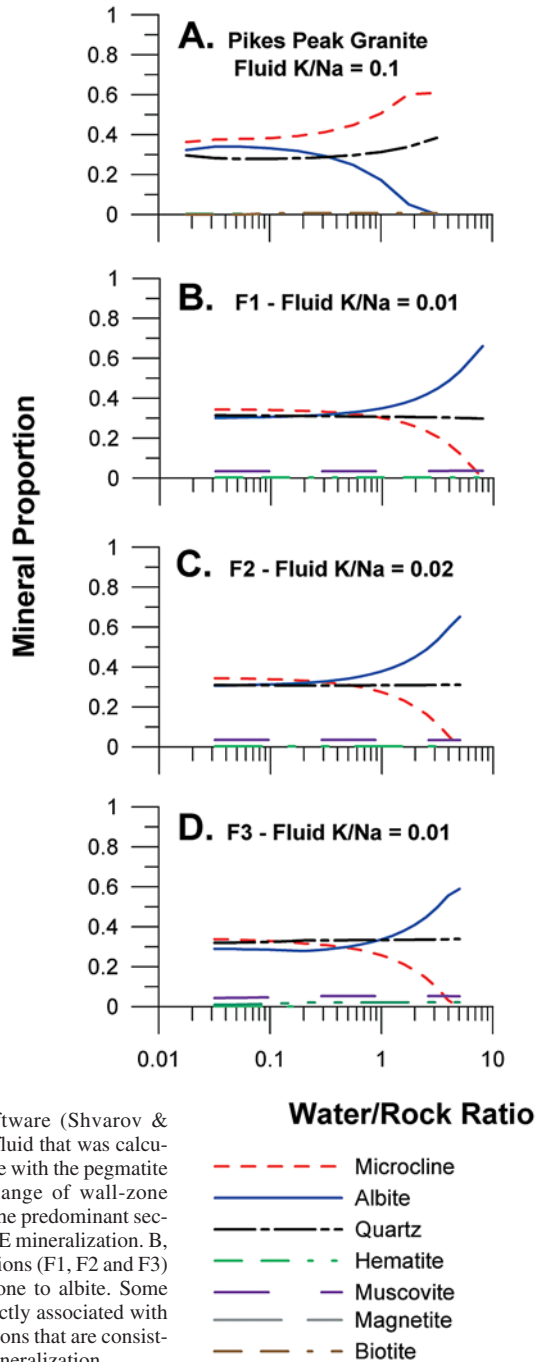


FIG. 12. Fluid-mineral reactions generated using HCh software (Shvarov & Bastrakov 1999). A. This graph represents the reaction of a fluid that was calculated to be in chemical equilibrium with the Pikes Peak granite with the pegmatite wall-zone. Such an interaction would result in the exchange of wall-zone microcline perthite to microcline rather than albite, which is the predominant secondary mineral associated with the hydrothermal fluorite-REE mineralization. B, C and D. In contrast, reaction of quartz-hosted fluid compositions (F1, F2 and F3) with the wall-zone would result in alteration of the wall zone to albite. Some quartz-hosted fluid compositions (*i.e.*, F2), although not directly associated with the fluorite-REE mineralization, apparently reflect compositions that are consistent with the alteration that accompanies the fluorite-REE mineralization.

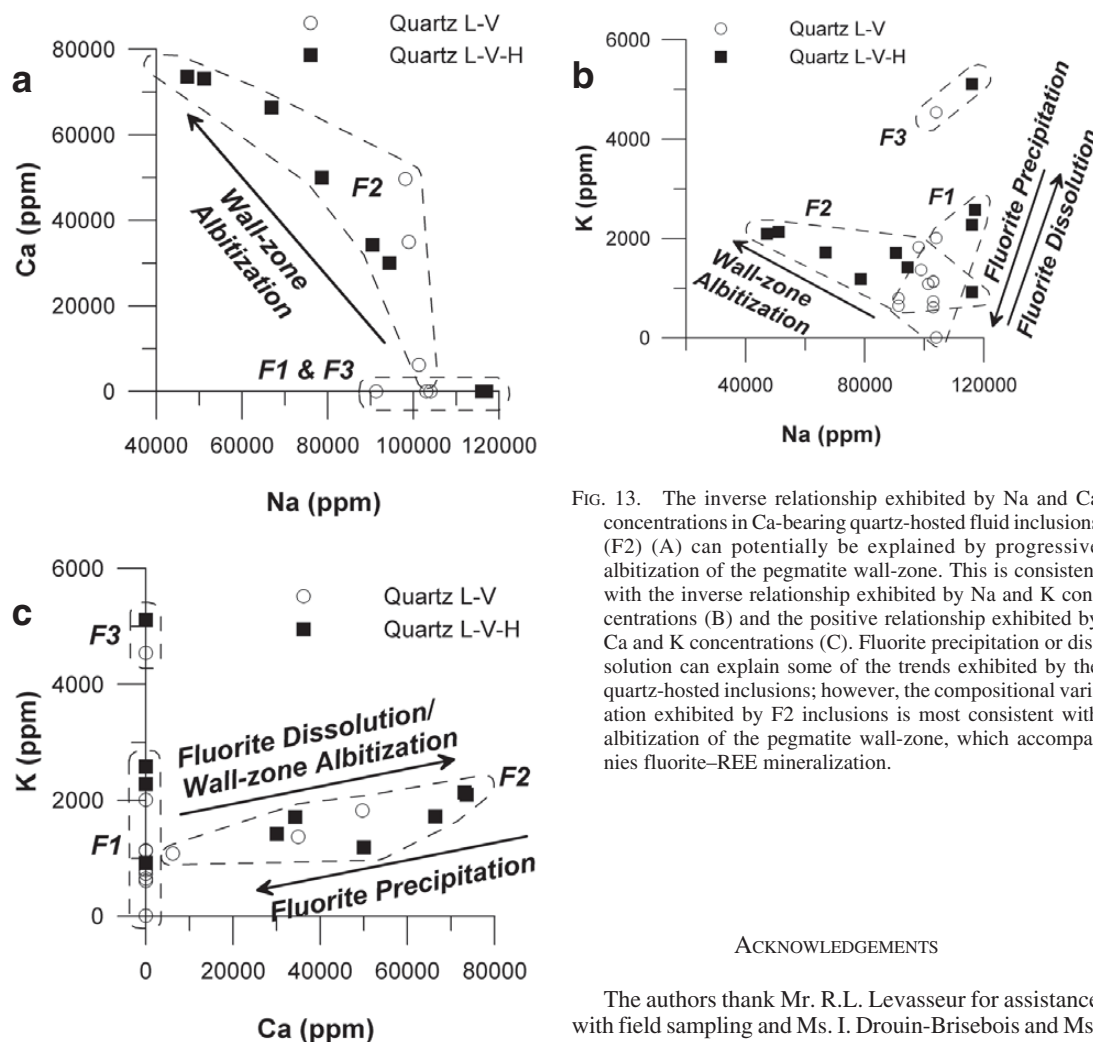


FIG. 13. The inverse relationship exhibited by Na and Ca concentrations in Ca-bearing quartz-hosted fluid inclusions (F2) (A) can potentially be explained by progressive albitization of the pegmatite wall-zone. This is consistent with the inverse relationship exhibited by Na and K concentrations (B) and the positive relationship exhibited by Ca and K concentrations (C). Fluorite precipitation or dissolution can explain some of the trends exhibited by the quartz-hosted inclusions; however, the compositional variation exhibited by F2 inclusions is most consistent with albitization of the pegmatite wall-zone, which accompanies fluorite-REE mineralization.

ACKNOWLEDGEMENTS

The authors thank Mr. R.L. Levasseur for assistance with field sampling and Ms. I. Drouin-Brisebois and Ms. M. Flore for assistance with microthermometry. Drs. D.J. Kontak and A.J. Anderson are thanked for their insightful reviews of an earlier version of this manuscript. We thank R.F. Martin for his editorial handling of the manuscript. This research was funded by NSERC discovery grants to AEW-J, IMS and BJB and by a McGill Graduate Student Fellowship and SEG Student Travel Grant to JEG.

REFERENCES

AUDÉTAT, A., GÜNTHER, D. & HEINRICH, C.A. (1998): Formation of a magmatic-hydrothermal ore deposits: insights with LA-ICP-MS analysis of fluid inclusions. *Science* **279**, 2091-2094.

\_\_\_\_\_, \_\_\_\_\_ & \_\_\_\_\_ (2000): Causes for large-scale metal zonation around mineralization plutons: fluid inclusion LA-ICP-MS evidence from the Mole granite, Australia. *Econ. Geol.* **95**, 1563-1581.

been directly responsible for fluorite deposition, may be the result of fluorite dissolution or pegmatite wall-zone albitization. The lack of a direct association of F2 with fluorite precipitation, however, makes this association speculative.

4) The approach used by Heinrich *et al.* (1992, 2003) to correct  $Na_{MT}$  using halite-dissolution temperatures, is valid only for temperatures in excess of approximately 300°C. At lower temperatures, a graphical solution using the data of Vanko *et al.* (1988) or Williams-Jones & Samson (1990) is necessary; which dataset is selected depends on how well the isotherms are defined in the range of T relevant to the study. Improvements in the topology of the liquidus surface in the range of T from 100 to 300°C would improve the accuracy of the determinations made using this graphical solution.

- BARKER, F., WONES, D.R., SHARP, W.N. & DESBOROUGH, G.A. (1975): The Pikes Peak batholith, Colorado Front Range, and a model for the origin of the gabbro – anorthosite – syenite – potassic granite suite. *Precamb. Res.* **2**, 97-160.
- BODNAR, R.J. (1993): Revised equation and table for determining the freezing point depression of H<sub>2</sub>O–NaCl solutions. *Geochim. Cosmochim. Acta* **57**, 683-684.
- BREWSTER, R.H. (1986): *The Distribution and Chemistry of Rare-Earth Minerals in the South Platte Pegmatite District, Colorado, and their Genetic Implications*. M.S. thesis, Univ. New Orleans, New Orleans, Louisiana.
- BÜHN, B., SCHNEIDER, J., DULSKI, P. & RANKIN, A.H. (2003): Fluid–rock interaction during progressive migration of carbonatitic fluids, derived from small-scale trace element and Sr, Pb isotope distribution in hydrothermal fluorite. *Geochim. Cosmochim. Acta* **67**, 4577-4595.
- GAGNON, J.E., SAMSON, I.M. & FRYER, B.J. (2003a): LA–ICP–MS analysis of fluid inclusions. In *The Analysis and Interpretation of Fluid Inclusions* (I. Samson, A. Anderson & D. Marshall, eds.). *Mineral. Assoc. Can., Short Course Vol. 32*, 12-1 – 12-32.
- \_\_\_\_\_, \_\_\_\_\_, \_\_\_\_\_ & WILLIAMS-JONES, A.E. (2002): Hydrothermal fluids in NYF pegmatites, South Platte, Colorado – preliminary insights from LA–ICP–MS analysis of quartz- and fluorite-hosted fluid inclusions. *Eighth Pan-American Conf. on Research on Fluid Inclusions, Program with Abstr.*, 25-27.
- \_\_\_\_\_, \_\_\_\_\_, \_\_\_\_\_ & \_\_\_\_\_ (2003b): Compositional heterogeneity in fluorite and the genesis of fluorite deposits: insights from LA–ICP–MS analysis. *Can. Mineral.* **41**, 365-382.
- GÜNTHER, D., AUDÉTAT, A., FRISCHKNECHT, R. & HEINRICH, C.A. (1998): Quantitative analysis of major, minor and trace elements in fluid inclusions using laser ablation – inductively coupled plasma – mass spectrometry (LA–ICP–MS). *J. Anal. Atom. Spectrom.* **13**, 263-270.
- HALTER, W. E., PETTKE, T., HEINRICH, C.A. & ROTHENRUTISHAUSER, B. (2002): Major to trace element analysis of melt inclusions by laser-ablation ICP–MS: methods of quantification. *Chem. Geol.* **183**, 63-86.
- HEDGE, C.E. (1970): Whole rock Rb–Sr age of the Pikes Peak Batholith, Colorado. *U.S. Geol. Surv., Prof. Pap.* **700B**, 86-89.
- HEINRICH, C.A., GÜNTHER, D., AUDÉTAT, A., ULRICH, T. & FRISCHKNECHT, R. (1999): Metal fractionation between magmatic brine and vapor, determined by microanalysis of fluid inclusions. *Geology* **27**, 755-758.
- \_\_\_\_\_, PETTKE, T., HALTER, W., AIGNER, M., AUDÉTAT, A., GÜNTHER, D., HATTENDORF, B., BLEINER, D., GUILLONG, M. & HORN, I. (2003): Quantitative multi-element analysis of minerals, fluid and melt inclusions by laser-ablation inductively-coupled – plasma mass-spectrometry. *Geochim. Cosmochim. Acta* **67**, 3473-3496.
- \_\_\_\_\_, RYAN, C.G., MERNAGH, T.P. & EADINGTON, P.J. (1992): Segregation of ore metals between magmatic brine and vapor: a fluid inclusion study using PIXE micro-analysis. *Econ. Geol.* **87**, 1566-1583.
- HUTCHINSON, R.M. (1960): Structure and petrology of north end of Pikes Peak batholith, Colorado. In *Guide to the Geology of Colorado* (R.J. Weimer & J.D. Haun, eds.). *Geological Society of America, Rocky Mountain Association of Geologists and Colorado Scientific Society*, 170-180.
- JOHNSON, J.W., OELKERS, E.H. & HELGESON, H.C. (1992): SUPCRT92: a software package for calculating the standard molal thermodynamic properties of minerals, gases, aqueous species and reactions from 1 to 5000 bars and 0° to 1000°C. *Comput. & Geosci.* **18**, 899-947.
- LANDTWING, M.R., REDMOND, P.B., EINAUDI, M.T., HEINRICH, C.A., HALTER, W.E. & PETTKE, T. (2002): Veining, timing of sulphide deposition and fluid evolution at the Bingham Cu–Au–Mo–Ag porphyry deposit – fluid inclusion LA–ICP–MS results. *Eighth Biennial Pan-American Conf. on Research on Fluid Inclusions, Program Abstr.*, 49-50 (abstr.).
- LEVASSEUR, R.L. (1997): *Fluid Inclusion Studies of Rare Element Pegmatites, South Platte District, Colorado*. M.Sc. thesis, Univ. of Windsor, Windsor, Ontario.
- \_\_\_\_\_, \_\_\_\_\_ & SAMSON, I.M. (1996): Fluid inclusion characteristics of REE–Y–Nb pegmatites, South Platte District, Colorado. *Geol. Assoc. Can. – Mineral. Assoc. Can., Program Abstr.* **21**, A56.
- LONGERICH, H.P., JACKSON, S.E. & GÜNTHER, D. (1996): Laser ablation inductively coupled plasma mass spectrometric transient signal data acquisition and analyte concentration calculation. *J. Anal. Atom. Spectrom.* **11**, 899-904.
- MÜLLER, B., FRISCHKNECHT, R., SEWARD, T.M., HEINRICH, C.A. & GALLEGOS, W.C. (2001): A fluid inclusion reconnaissance study of the Huanuni tin deposit (Bolivia), using LA–ICP–MS micro-analysis. *Mineral. Deposita* **36**, 680-688.
- OAKES, C.S., BODNAR, R.J. & SIMONSON, J.M. (1990): The system NaCl–CaCl<sub>2</sub>–H<sub>2</sub>O. I. The vapour-saturated ice liquidus. *Geochim. Cosmochim. Acta* **54**, 603-610.
- RICHARDSON C.K. & HOLLAND, H.D. (1979): Fluorite deposition in hydrothermal systems. *Geochim. Cosmochim. Acta* **43**, 1327-1335.
- SALVI, S. & WILLIAMS-JONES, A.E. (1990): The role of hydrothermal processes in the granite-hosted Zr, Y, REE deposit at Strange Lake, Quebec/Labrador: evidence from fluid inclusions. *Geochim. Cosmochim. Acta* **54**, 2403-2418.
- \_\_\_\_\_, \_\_\_\_\_ (1992): Reduced orthomagmatic C–O–H–NaCl fluids in the Strange Lake rare-metal granitic complex, Quebec/Labrador, Canada. *Eur. J. Mineral.* **4**, 1155-1174.
- SAMSON, I.M., KERR, I.D. & GRAF, C. (2001): The Rock Canyon Creek fluorite–REE deposit, British Columbia. In *In-*

- dustrial Minerals in Canada. *Can. Inst. Mining Metall., Spec. Vol.* **53**, 1-10.
- SHEPHERD, T.J., AYORA, C., CENDÓN, D.I., CHENERY, S.R. & MOISSETTE, A. (1998): Quantitative solute analysis of single fluid inclusions in halite by LA-ICP-MS and cryo-SEM-EDS: complementary microbeam techniques. *Eur. J. Mineral.* **10**, 1097-1108.
- SHOCK, E.L. (1998): Sequential access thermodynamic datafile for SUPCRIT92. Arizona State University, Department of Geological Sciences, GEOPIG database.
- SHVAROV, YU.V. & BASTRAKOV, E.N. (1999): HCh: a software package for geochemical equilibrium modelling. User's guide. *Aust. Geol. Surv. Org., Record* **1999/25**.
- SIMMONS, W.B. & HEINRICH, E.W. (1970): Rare-earth - fluorine pegmatites of the South Platte district, Jefferson County, Colorado. *Geol. Assoc. Can. - Mineral. Assoc. Can., Program Abstr.* 48-49.
- \_\_\_\_\_ & \_\_\_\_\_ (1980): Rare-earth pegmatites of the South Platte district, Colorado, *Colorado Geol. Surv., Dep. Nat. Resources, Resource Ser.* **11**.
- \_\_\_\_\_, LEE, M.T. & BREWSTER, R.H. (1987): Geochemistry and evolution of the South Platte granite-pegmatite system, Jefferson County, Colorado. *Geochim. Cosmochim. Acta* **51**, 455-471.
- SMITH, D.R., NOBLETT, J., WOBUS, R.A., UNRUH, D., DOUGLASS, J., BEANE, R., DAVIS, C., GOLDMAN, S., KAY, G., GUSTAVSON, B., SALTOUN, B. & STEWART, J. (1999): Petrology and geochemistry of late-stage intrusions of the A-type, mid-Proterozoic Pikes Peak batholith (central Colorado, USA): implications for petrogenetic models. *Precamb. Res.* **98**, 271-305.
- STERNER, S.M., HALL, D.L. & BODNAR, R.J. (1988): Synthetic fluid inclusions. V. Solubility relations in the system NaCl-KCl-H<sub>2</sub>O under vapor-saturated conditions. *Geochim. Cosmochim. Acta* **52**, 989-1005.
- ULRICH, T., GÜNTHER, D. & HEINRICH, C.A. (1999): Gold concentrations of magmatic brines and the metal budget of porphyry copper deposits. *Nature* **399**, 676-679.
- VANKO, D.A., BODNAR, R.J. & STERNER, S.M. (1988): Synthetic fluid inclusions. VIII. Vapor-saturated halite solubility in part of the system NaCl-CaCl<sub>2</sub>-H<sub>2</sub>O, with application to fluid inclusions from oceanic hydrothermal systems. *Geochim. Cosmochim. Acta* **52**, 2451-2456.
- WILLIAMS-JONES, A.E. & SAMSON, I.M. (1990): Theoretical estimation of halite solubility in the system NaCl-CaCl<sub>2</sub>-H<sub>2</sub>O: applications to fluid inclusions. *Can. Mineral.* **28**, 299-304.
- \_\_\_\_\_, \_\_\_\_\_ & OLIVO, G.R. (2000): The genesis of hydrothermal fluorite-REE deposits in the Gallinas Mountains, New Mexico. *Econ. Geol.* **95**, 327-342.

Received April 1, 2004, revised manuscript accepted September 9, 2004.